

# **Fuel-Flexible Gasification-Combustion Technology for Production of H<sub>2</sub> and Sequestration-Ready CO<sub>2</sub>**

Annual Technical Progress Report 2003

Reporting Period:

October 1, 2002 – September 30, 2003

George Rizeq, Janice West, Arnaldo Frydman, Raul Subia, and Vladimir Zamansky (GEGR)  
Hana Loreth, Lubor Stonawski, Tomasz Wiltowski, Edwin Hippo, and Shashi Lalvani (SIU-C)

**October 2003**

DOE Award No. DE-FC26-00FT40974

GE Global Research  
(GEGR)  
18 Mason  
Irvine, CA 92618

## **DISCLAIMER**

“This report was prepared as an account of work sponsored by an agency of the United States Government. Neither the United States Government nor any agency thereof, nor any of their employees, makes any warranty, express or implied, or assumes any legal liability or responsibility for the accuracy, completeness, or usefulness of any information, apparatus, product, or process disclosed, or represents that its use would not infringe privately owned rights. Reference herein to any specific commercial product, process, or service by trade name, trademark, manufacturer, or otherwise does not necessarily constitute or imply its endorsement, recommendation, or favoring by the United States Government or any agency thereof. The views and opinions of authors expressed herein do not necessarily state or reflect those of the United States Government or any agency thereof.”

## **ABSTRACT**

It is expected that in the 21<sup>st</sup> century the Nation will continue to rely on fossil fuels for electricity, transportation, and chemicals. It will be necessary to improve both the process efficiency and environmental impact performance of fossil fuel utilization. GE Global Research (GEGR) has developed an innovative fuel-flexible Unmixed Fuel Processor (UFP) technology to produce H<sub>2</sub>, power, and sequestration-ready CO<sub>2</sub> from coal and other solid fuels. The UFP module offers the potential for reduced cost, increased process efficiency relative to conventional gasification and combustion systems, and near-zero pollutant emissions including NO<sub>x</sub>. GEGR (prime contractor) was awarded a contract from U.S. DOE NETL to develop the UFP technology. Work on this Phase I program started on October 1, 2000. The project team includes GEGR, Southern Illinois University at Carbondale (SIU-C), California Energy Commission (CEC), and T. R. Miles, Technical Consultants, Inc.

In the UFP technology, coal and air are simultaneously converted into separate streams of (1) high-purity hydrogen that can be utilized in fuel cells or turbines, (2) sequestration-ready CO<sub>2</sub>, and (3) high temperature/pressure vitiated air to produce electricity in a gas turbine. The process produces near-zero emissions and, based on Aspen Plus process modeling, has an estimated process efficiency of 6% higher than IGCC with conventional CO<sub>2</sub> separation. The current R&D program will determine the feasibility of the integrated UFP technology through pilot-scale testing, and will investigate operating conditions that maximize separation of CO<sub>2</sub> and pollutants from the vent gas, while simultaneously maximizing coal conversion efficiency and hydrogen production. The program integrates experimental testing, modeling and economic studies to demonstrate the UFP technology.

This is the third annual technical progress report for the UFP program supported by U.S. DOE NETL (Contract No. DE-FC26-00FT40974). This report summarizes program accomplishments for the period starting October 1, 2002 and ending September 30, 2003. The report includes an introduction summarizing the UFP technology, main program tasks, and program objectives; it also provides a summary of program activities and accomplishments covering progress in tasks including lab-scale experimental testing, bench-scale experimental testing, process modeling, pilot-scale system design and assembly, and program management.

## TABLE OF CONTENTS

|  |           |
|--|-----------|
| <b>DISCLAIMER .....</b>  | <b>2</b>  |
| <b>ABSTRACT .....</b>  | <b>3</b>  |
| <b>LIST OF TABLES.....</b>   | <b>5</b>  |
| <b>LIST OF FIGURES.....</b>  | <b>6</b>  |
| <b>EXECUTIVE SUMMARY .....</b>   | <b>7</b>  |
| <b>1.0 INTRODUCTION.....</b>   | <b>9</b>  |
| 1.1 PROGRAM OBJECTIVES .....   | 9         |
| 1.2 UFP TECHNOLOGY.....  | 10        |
| 1.3 PROJECT PLAN .....   | 10        |
| <b>2.0 PROGRAM PLANNING AND MANAGEMENT .....</b>                                   | <b>11</b> |
| <b>3.0 EXPERIMENTAL .....</b>  | <b>13</b> |
| 3.1 LABORATORY-SCALE TESTING .....   | 13        |
| 3.1.1 Coal Gasification Experiments .....  | 13        |
| 3.1.2 OTM Characterization Experiments .....                                       | 13        |
| 3.2 BENCH-SCALE TESTING.....   | 15        |
| <b>4.0 RESULTS AND DISCUSSION.....</b>   | <b>17</b> |
| 4.1 LABORATORY-SCALE TESTING RESULTS .....   | 17        |
| 4.1.1 Coal Gasification Results.....   | 17        |
| 4.1.2 OTM Characterization Results .....   | 19        |
| 4.2 BENCH-SCALE TESTING RESULTS.....   | 20        |
| 4.3 ENGINEERING AND MODELING STUDIES.....  | 22        |
| 4.3.1 Pilot-Scale System Process Modeling .....                                    | 22        |
| 4.3.2 UFP Integrated System Process Modeling / Comparison with IGCC (Task 8) ..... | 25        |
| Difference in energy utilization.....  | 29        |
| 4.4 PILOT PLANT DESIGN & ASSEMBLY .....  | 30        |
| 4.4.1 Safety Analysis .....  | 30        |
| 4.4.2 Reactor Design and Construction .....  | 30        |
| 4.4.3 Coal, Steam and Air Feeding Systems.....                                     | 31        |
| 4.4.4 Solids Transfer System .....   | 33        |
| 4.4.5 Auxiliary Systems.....   | 33        |
| 4.4.6 UFP Pilot Plant Layout .....   | 34        |
| 4.4.7 Control, Monitoring and Analysis Systems .....                               | 35        |
| <b>5.0 CONCLUSIONS.....</b>  | <b>37</b> |
| <b>6.0 FUTURE WORK .....</b>   | <b>39</b> |
| <b>7.0 PUBLICATIONS AND PRESENTATIONS .....</b>                                    | <b>41</b> |
| <b>8.0 REFERENCES.....</b>   | <b>43</b> |
| <b>LIST OF ACRONYMS AND ABBREVIATIONS .....</b>                                    | <b>44</b> |

## LIST OF TABLES

|          |  |    |
|----------|--|----|
| Table 1  | Main tasks of the UFP program. ....  | 11 |
| Table 2  | Test matrix for investigation of OTM behavior .....  | 14 |
| Table 3  | Selected solid-state reaction rate equations .....   | 15 |
| Table 4  | OTM test conditions for full test matrix .....   | 16 |
| Table 5  | Product gas composition and volume results obtained for tests conducted with a variety of bed:coal ratios and bed compositions ..... | 17 |
| Table 6  | Results from lab-scale high temperature coal gasification tests .....  | 18 |
| Table 7  | OTM test conditions and results for full test matrix .....   | 21 |
| Table 8  | Comparison of transfer function predictions with actual experimental data .....  | 21 |
| Table 9  | Input parameters for UFP pilot-scale simulation .....  | 23 |
| Table 10 | Major process modeling assumptions for the full-scale UFP integrated with combined cycle plant .....                                 | 27 |
| Table 11 | Comparison of the efficiencies for the IGCC process and the UFP technology .....   | 29 |

## LIST OF FIGURES

|           |  |    |
|-----------|--|----|
| Figure 1  | Conceptual design of the UFP technology.....   | 10 |
| Figure 2  | Lab-scale coal gasification results: product volume and $H_2$ volume at different bed compositions .....   | 18 |
| Figure 3  | Conversion degree as a function of time for a 90% $N_2$ , 10% $CO$ mixture at a variety of temperatures.....   | 19 |
| Figure 4  | Conversion degree as a function of time for a 90% $N_2$ , 10% $H_2$ mixture at a variety of temperatures.....  | 19 |
| Figure 5  | Conversion degree as a function of time for a 90% $N_2$ , 5.7% $CO$ , 4.3% $H_2$ mixture at a variety of temperatures.....   | 20 |
| Figure 6  | Conversion degree as a function of time for a 90% $N_2$ , 2% $CO$ , 8% $H_2$ mixture at a variety of temperatures .....  | 20 |
| Figure 7  | Transfer function predictions of OTM reduction as a function of $CO$ concentration and GHSV at 10% $H_2$ concentration .....   | 21 |
| Figure 8  | ASPEN simulation process flow diagram for UFP pilot-scale system.....  | 23 |
| Figure 9  | Contour plots that represent the temperature as a function of coal conversion and initial OTM bed fraction ( $OTM_1$ ) at a coal feed rate of 25 lb/hr .....   | 24 |
| Figure 10 | The impact of initial OTM fraction and coal conversion on four key performance indicators ( $H_2$ product concentration in R1, fraction of C in coal separated as $CO_2$ in R2, $H_2$ concentration in R2, and $CO_2$ concentration in R3) at a coal feed rate of 25 lb/hr ..... | 25 |
| Figure 11 | Simplified process flow diagram for UFP technology integrated with combined cycle plant for co-production of hydrogen and electricity from coal.....   | 26 |
| Figure 12 | Process flow diagram for the 3-pressure reheat steam cycle .....   | 26 |
| Figure 13 | Process flow diagrams for (A) Typical IGCC process with $CO_2$ separation and (B) UFP process integrated with the combined cycle plant .....   | 28 |
| Figure 14 | Hydrostatic test of Reactor 2.....   | 30 |
| Figure 15 | Reactor 1 shell with two-cast refractory layers.....   | 30 |
| Figure 16 | Pilot-scale distributor plate design with detail of nozzle bolts .....   | 31 |
| Figure 17 | Photo of three pilot-scale reactors mounted on stand .....   | 31 |
| Figure 18 | Photo and schematic diagram of second-stage superheater: electric furnace and heating coil.....  | 32 |
| Figure 19 | High-pressure air feeding system: high pressure and low-pressure receiver tanks ....   | 32 |
| Figure 20 | Cold flow model: 3 circulating fluidized beds.....   | 33 |
| Figure 21 | Cutaway view of Reactor 2 (see 3-reactor inset) showing solids transfer ducts and reactor internals.....   | 33 |
| Figure 22 | Emissions control system: afterburner, quench, and scrubber in series .....  | 34 |
| Figure 23 | Layout of pilot-scale system .....   | 34 |
| Figure 24 | Process and instrumentation diagram for the pilot-scale system .....   | 36 |
| Figure 25 | Side view of pilot-scale system with three reactors, scaffolding and second-stage superheaters shown .....   | 40 |

## **EXECUTIVE SUMMARY**

This is the third annual technical progress report for the UFP program supported by U.S. DOE NETL (Contract No. DE-FC26-00FT40974). This report summarizes program accomplishments for the period starting October 1, 2002 and ending September 30, 2003. The report provides a description of the technology concept and a summary of program activities and accomplishments covering progress in tasks including lab-scale experimental testing, bench-scale experimental testing, process modeling, pilot-scale system design and assembly, and program management.

In the UFP technology, coal/opportunity fuels and air are simultaneously converted into separate streams of (1) pure hydrogen that can be utilized in fuel cells, (2) sequestration-ready CO<sub>2</sub>, and (3) high temperature/pressure oxygen-depleted air to produce electricity in a gas turbine. The process is highly efficient relative to conventional electricity producing technologies and produces near-zero emissions. This R&D program will determine the operating conditions that maximize separation of CO<sub>2</sub> and pollutants from the vent gas, while simultaneously maximizing coal conversion to electricity efficiency and hydrogen production. The program integrates lab-, bench- and pilot-scale studies to demonstrate the UFP technology.

Work conducted in the third year of the program has included the design of components and subsystems of the pilot-scale facility, planning for assembly of the pilot plant, bench-scale testing of key UFP processes, and additional experimental analysis conducted at lab scale.

The lab-scale effort in the third year has included experimental investigations into both coal gasification and OTM reduction behavior. Coal gasification experiments provided data on the effectiveness of the CO<sub>2</sub>-absorbing material (CAM) at removing CO<sub>2</sub> from the H<sub>2</sub>-rich product stream. Other coal gasification experiments provided insight into the impact of bed composition on UFP performance. TGA experiments were conducted to evaluate and quantify the kinetics of OTM reduction and OTM speciation as a function of temperature. This information will provide key kinetic parameters for integration in process and kinetic modeling of the system. The residence times of solids in the pilot-scale system will be set based on kinetic modeling results to ensure that sufficient time for reaction.

Bench-scale experiments conducted in the third year resulted in the development of a transfer function relating OTM reduction to GHSV and inlet concentration. This transfer function was used to identify a set of operating conditions that would provide optimized OTM reduction results. Additional testing was conducted to confirm the predicted performance at the optimized conditions, and the transfer function was updated to include all experimental results. In the expected region of operation of the pilot-scale system, the transfer function predicts reduction of up to 20% of the OTM present in the bed.

Modeling work conducted in the current reporting period has focused on development of two ASPEN process models: a model of the pilot-scale system, and a model of the full-scale UFP system integrated with a combined cycle plant. The pilot-scale UFP model was used to assist in identifying initial pilot plant operating conditions for system shakedown. Key model input parameters include the coal feed rate, extent of coal conversion in Reactor 1, and the initial bed composition (OTM:CAM ratio). Contour plots were used to identify operating conditions for

each of the three reactors that satisfy operating requirements as well as provide good performance. Key performance variables include H<sub>2</sub> purity in R1 and CO<sub>2</sub> separation in R2. The full-scale integrated UFP model was used to estimate performance for comparison with competing technologies and to provide the inputs for preliminary economic analysis. Preliminary results obtained with the model show an efficiency improvement of 6% over IGCC. It is expected that further model optimization will result in a 10% efficiency improvement.

The pilot-scale effort has progressed beyond the design of the system and into construction and shakedown testing of individual system components. Delays in obtaining a construction and operating permit have prevented the system from being assembled as a single unit, but planning activities have continued to ensure a streamlined assembly phase. Work conducted in the third program year has involved finalizing designs, obtaining equipment, and conducting shakedown testing of individual subsystems. In addition, care has been taken to ensure that instrumentation is in place to both allow effective control of the system as well as monitor key performance indicators.

A detailed safety analysis was conducted for the entire pilot-scale system, focusing on potential hazards and their mitigation, which have been considered in the standard and emergency operating procedures developed. The reactor designs have been reviewed, and the three reactors were manufactured and cast with two refractory layers. The systems to feed air, steam and coal were specified and manufactured. The air and coal systems have been partly assembled and tested, while the steam boiler system has been built and is being tested by the manufacturer. The solids transfer system was tested in a cold-flow model and the pilot-scale solids transfer ducts have been manufactured and cast with refractory. The emission control system, which includes an afterburner and scrubber with quench have been designed to prevent the emission of air pollutants during operation of the non-integrated system. The afterburner, quench and scrubber have been constructed and are awaiting shakedown testing. Instrumentation has been specified to meet the harsh operating conditions of the pilot plant, and is on site and awaiting assembly. The data acquisition and control system is being designed to allow safe and effective operation of the pilot plant as well as the monitoring of key variables that will be used to assess actual pilot plant performance.

## 1.0 INTRODUCTION

Electricity produced from hydrogen in fuel cells can be highly efficient relative to competing technologies and has the potential to be virtually pollution free. Thus, fuel cells may become an ideal solution to many of this nation's energy needs if one has a satisfactory process for producing hydrogen from available energy resources such as coal, and low-cost alternative feedstocks such as biomass.

This UFP program addresses a novel, energy-efficient, and near-zero pollution concept for converting coal into separate streams of hydrogen, vitiated air, and sequestration-ready  $CO_2$ . The technology module comprising this concept will be referred to as the *Unmixed Fuel Processor (UFP)* throughout this report. When commercialized, the UFP technology may become one of the cornerstone technologies to fulfill the DOE's future energy plant objectives of efficiently and economically producing energy and hydrogen from coal with utilization of opportunity feedstocks.

The UFP technology is energy efficient because a large portion of the energy in the coal feed leaves the UFP module as hydrogen and the rest as high-pressure, high-temperature gas that can power a gas turbine. The combination of producing hydrogen and electricity via a gas turbine is highly efficient, meets all objectives of DOE future energy plants, and makes the process product flexible. That is, the UFP module will be able to adjust the ratio at which it produces hydrogen and electricity in order to match changing demand.

General Electric Global Research (GEGR) is the primary contractor for the UFP program under a contract from U.S. DOE NETL (Contact No. DE-FC26-00FT40974). Other project team members include Southern Illinois University at Carbondale (SIU-C), California Energy Commission (CEC), and T. R. Miles, Technical Consultants, Inc. The UFP project integrates lab, bench and pilot-scale studies to demonstrate the UFP technology. Engineering studies and analytical modeling are being performed in conjunction with the experimental program to develop the design tools necessary for scaling up the UFP technology to the demonstration phase. The remainder of this section presents objectives, concept, and main tasks of the UFP program.

### 1.1 Program Objectives

The primary objectives of the UFP program are to:

- Demonstrate and establish the chemistry of the UFP technology, measure kinetic parameters of individual process steps, and identify fundamental processes affecting process economics.
- Design and develop bench- and pilot-scale systems to test the UFP technology under dynamic conditions and estimate the overall system efficiency for the design.
- Develop kinetic and dynamic computational models of the individual process steps.
- Determine operating conditions that maximize separation of  $CO_2$  and pollutants from vent gas, while simultaneously maximizing coal/opportunity fuels conversion and  $H_2$  production.
- Integrate the UFP module into Vision 21 plant design and optimize work cycle efficiency.
- Determine extent of technical/economical viability & commercial potential of UFP module.

## 1.2 UFP technology

The conceptual design of the UFP technology is depicted in Figure 1. The UFP technology makes use of three circulating fluidized bed reactors containing  $CO_2$  absorbing material (CAM) and oxygen transfer material (OTM), as shown in Figure 1. Coal is partially gasified with steam in the first reactor, producing  $H_2$ , CO and  $CO_2$ . As  $CO_2$  is absorbed by the CAM, CO is also depleted from the gas phase via the water-gas shift reaction. Thus, the first reactor produces a  $H_2$ -rich product stream suitable for use in liquefaction, fuel cells, or turbines.

Gasification of the char, transferred from the first reactor, is completed with steam fluidization in the second reactor. The oxygen transfer material is reduced as it provides the oxygen needed to oxidize CO to  $CO_2$  and  $H_2$  to  $H_2O$ . The  $CO_2$  sorbent is regenerated as the hot moving material from the third reactor enters the second reactor.

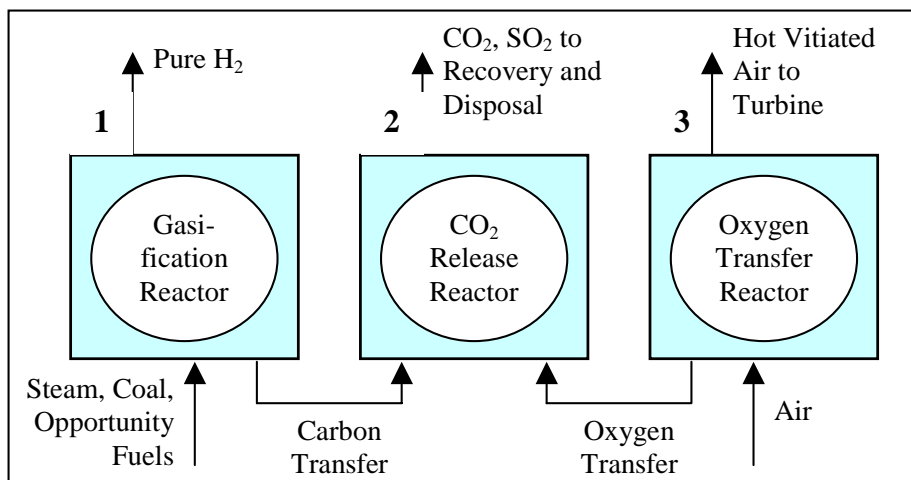


Figure 1. Conceptual design of the UFP technology.

This increases the bed temperature forcing the release of  $CO_2$  from the sorbent, generating a  $CO_2$ -rich product stream suitable for sequestration.

Air fed to the third reactor re-oxidizes the oxygen transfer material via a highly exothermic reaction that consumes the oxygen in the air fed. Thus, Reactor 3 produces oxygen-depleted air for a gas turbine as well as generating heat that is transferred to the first and second reactors via solids transfer.

Solids transfer occurs between all three reactors, allowing for the regeneration and recirculation of both the  $CO_2$  sorbent and the oxygen transfer material. Periodically, ash and bed materials will be removed from the system and replaced with fresh bed materials to reduce the amount of ash in the system and increase the effectiveness of the bed materials.

## 1.3 Project Plan

Work on tasks planned for the UFP project (Table 1) started in October 2000. The project was originally scheduled for completion in three years, but a nine-month no-cost extension granted by the DOE in August 2003, extended the completion date until June 2004. This extension was necessary due to delays in obtaining South Coast AQMD permit to construct and operate the pilot plant. The success of the UFP program depends on the efficient execution of the various research tasks outlined in Table 1 and on meeting the program objectives summarized above.

## 2.0 PROGRAM PLANNING AND MANAGEMENT

Program planning activities have focused on meeting the objectives of the program as stated previously. GEGR has made use of several GE methodologies to obtain desired results and systematically conduct program design, construction and testing activities. Methodologies utilized in this program include New Technology Introduction (NTI) and Design For Six Sigma (DFSS). The NTI program is a detailed and systematic methodology used by GE to identify market drivers, and continually ensure that the program will meet both current and future market needs. The NTI program is also strongly coupled with the DFSS and other quality programs, providing structure to the design process and ensuring that the design accomplished through regular program reviews, detailed design reviews, market assessments, planning and decision tools, and specific quality projects aimed at identifying system features and attributes that are critical to quality (CTQ) for customers.

The project team meets weekly to assess progress, distribute workload, and identify and remove potential roadblocks. An expanded NTI project team that includes senior management and other expert personnel also meets biweekly to gauge progress and ensure that adequate company resources are allocated and technical issues resolved to allow steady progress toward program objectives.

Program management activities also involve continuous oversight of program expenditures. This includes monthly review of actual expenditures and monthly projections of labor, equipment, contractor costs, and materials costs.

Technology transfer and networking with experts in the advanced power generation field is an important and ongoing part of project management. Team members continue to seek out

Table 1. Main tasks of the UFP program.

| Task   | Task Description   |
|--|--|
| Lab-Scale Experiments – Fundamentals<br><i>Task 1</i>                          | Design & assembly<br>Demonstration of chemical processes<br>Sulfur chemistry   |
| Bench-Scale Test Facility & Testing<br><br><i>Tasks 2 &amp; 3</i>              | Bench test facility design<br>Subsystems procurement & assembly<br>Bench test facility shakedown<br>Reactor design testing<br>Parametric evaluation<br>Fuel-flexibility evaluation<br>Pilot operation support  |
| Engineering & Modeling Studies<br><br><i>Task 4</i>                            | Opportunity fuels resource assessment<br>Preliminary economic assessment<br>Kinetic & process modeling<br>Integration into Vision 21 plant<br>Pilot plant control development  |
| Pilot Plant Design, Assembly & Demonstration<br><br><i>Tasks 5, 6, &amp; 7</i> | Process design<br>Subsystems specification/procurement<br>Reactor design & review<br>Reactors manufacture<br>Components testing<br>Pilot plant assembly<br>Operational shakedown modifications<br>Operational evaluation<br>Fuel-flexibility evaluation<br>Performance testing |
| Vision 21 Plant Systems Analysis<br><i>Task 8</i>                              | Preliminary Vision 21 module design<br>Vision 21 plant integration<br>Economic & market assessment   |
| Project Management<br><i>Task 9</i>  | Management, reporting, & technology transfer   |

opportunities to present the UFP technology and progress at technical conferences. During the third year, technical papers were presented at the Twentieth Annual International Pittsburgh Coal Conference in Pittsburgh, PA as well as the Gasification Technologies 2003 Conference in San Francisco, CA. GEGR's UFP technology team hosted a program review meeting for several U.S. DOE representatives at GEGR's offices in Irvine, CA on Wednesday, January 8, 2003. A simultaneous videoconference with the DOE NETL office in Pittsburgh allowed the participation of DOE personnel who could not travel to Irvine. The goals of the meeting were to review GEGR's progress on the UFP program and discuss related technology development plans. The all-day meeting included eight GEGR presentations, one DOE presentation, discussions, a visit to GEGR Cold Flow Modeling Laboratory, and a visit to GEGR's Test Site to tour the UFP facilities and other R&D program facilities at the site. During the meeting, DOE and GEGR teams were engaged in fruitful discussions that helped in optimizing R&D work on the UFP tasks over the last year. GEGR progress on the UFP project and further development steps were discussed in detail.

During the last quarter, the GEGR UFP team made preparations for another review meeting with DOE representatives (Gary Stiegel, Stewart Clayton and Gil McGurl) to be held on October 16, 2003 at GEGR's offices in Irvine, CA. During the daylong meeting, the UFP engineering team will provide several overviews of the UFP technology including progress to date and planned technology development activities. Details of the October 16 meeting with DOE will be provided in the next quarterly report.

During the third program year, additional results from the experimental facilities were obtained, analyzed and used to assess operating characteristics of the UFP. Modeling studies have provided insight into the preferred operation of the pilot-scale system as well as the competitiveness of the technology as compared to IGCC. The laboratory-scale activities are being conducted by SIU in Carbondale, IL, while the bench-scale and pilot-scale systems are located at GEGR's test facility in Irvine, CA. Significant progress was made toward procurement and assembly of the pilot plant components.

## **3.0 EXPERIMENTAL**

### **3.1 LABORATORY-SCALE TESTING**

The primary objective of Task 1 is to perform a laboratory-scale demonstration of the individual chemical and physical processes involved in GEGR's fuel-flexible UFP technology. Specific objectives of Task 1 include:

- Support bench- and pilot-scale studies;
- Assist in process optimization and engineering analysis;
- Identify key kinetic and thermodynamic limitations of the process; and
- Verify the process parameters at laboratory scale.

Work conducted in the third year of this program included lab-scale assessments of coal gasification and OTM reduction, two key UFP processes. The coal gasification experiments were conducted in a high-temperature fluidized bed with a variety of bed compositions. The reduction of OTM was characterized using both thermogravimetric analyzer (TGA) experiments and high-temperature fluidized bed experiments.

#### **3.1.1 Coal Gasification Experiments**

Experiments were conducted in SIU's lab-scale fluidized bed system to assess the impact of varying OTM:CAM ratios and coal loading on hydrogen production and hydrogen purity during the coal gasification step (Reactor 1 conditions). Bed materials were placed in the high-pressure lab-scale reactor, which was then heated to the desired temperature under flowing nitrogen at atmospheric pressure. Steam was then introduced into the reactor and the nitrogen flow rate was adjusted to provide a flow rate equal to 15 times the minimum fluidization velocity and a composition of 85% steam and 15% nitrogen.

Coal samples were injected into the reactor using the nitrogen-driven solids delivery system. Immediately after coal injection, the outlet gas samples and the outlet volumetric flow rates were measured at one-minute intervals for 30 minutes. Gas samples were analyzed using a gas chromatograph (GOW-MAC 600). The concentration and volume of the gas produced is indicative of the effectiveness of the CAM sorbent and the extent of coal gasification. Good performance in the gasification step is characterized by production of a large amount of product gas rich in H<sub>2</sub>, especially in tests conducted with CAM beds. The impact of OTM on coal gasification was also of interest. Results from these tests are summarized in Section 4.1.

#### **3.1.2 OTM Characterization Experiments**

The reduction of OTM is a key UFP process that has been tested extensively in the lab-scale system. In order to characterize and quantify the behavior of OTM, a test matrix was developed that includes both TGA and fluidized bed experiments. This test matrix covers the operating range of interest for quantifying the kinetic behavior of OTM. These test runs are described in Table 2. The use of the same H<sub>2</sub>/CO ratio for both the TGA and fluidized bed tests will allow more meaningful comparison of their results.

Table 2. Test matrix for investigation of OTM behavior.

| Test # | Test type | Pressure (atm) | Bed mass (g) | Carrier gas                       |                          |         |                   | Temp range (°C) |
|--------|-----------|----------------|--------------|-----------------------------------|--------------------------|---------|-------------------|-----------------|
|        |           |                |              | Feed gas type                     | H <sub>2</sub> /CO ratio | Inert % | Total flow (SLPM) |                 |
| 1      | TGA       | 1              | 0.01         | H <sub>2</sub> /CO/N <sub>2</sub> | 1                        | 90      | 0.0275            | 700-900         |
| 2      | TGA       | 1              | 0.01         | H <sub>2</sub> /CO/N <sub>2</sub> | 0.75                     | 90      | 0.0275            | 700-900         |
| 3      | TGA       | 1              | 0.01         | H <sub>2</sub> /CO/N <sub>2</sub> | 0.5                      | 90      | 0.0275            | 700-900         |
| 4      | TGA       | 1              | 0.01         | H <sub>2</sub> /CO/N <sub>2</sub> | 0.25                     | 90      | 0.0275            | 700-900         |
| 5      | TGA       | 1              | 0.01         | H <sub>2</sub> /CO/N <sub>2</sub> | CO only                  | 90      | 0.2144            | 700-900         |
| 6      | TGA       | 1              | 0.01         | H <sub>2</sub> /CO/N <sub>2</sub> | H <sub>2</sub> only      | 90      | 0.2144            | 700-900         |
| 7      | FB        | 20             | 50           | H <sub>2</sub> /CO/N <sub>2</sub> | 1                        | 90      | 0.2144            | 700-900         |
| 8      | FB        | 20             | 50           | H <sub>2</sub> /CO/N <sub>2</sub> | 0.75                     | 90      | 0.2144            | 700-900         |
| 9      | FB        | 20             | 50           | H <sub>2</sub> /CO/N <sub>2</sub> | 0.5                      | 90      | 0.2144            | 700-900         |
| 10     | FB        | 20             | 50           | H <sub>2</sub> /CO/N <sub>2</sub> | 0.25                     | 90      | 0.2144            | 700-900         |
| 11     | FB        | 20             | 50           | H <sub>2</sub> /CO/N <sub>2</sub> | CO only                  | 90      | 0.2144            | 700-900         |
| 12     | FB        | 20             | 50           | H <sub>2</sub> /CO/N <sub>2</sub> | H <sub>2</sub> only      | 90      | 0.2144            | 700-900         |
| 13     | FB        | 20             | 50           | H <sub>2</sub> /CO/steam          | 1                        | 90      | 0.2144            | 700-900         |
| 14     | FB        | 20             | 50           | H <sub>2</sub> /CO/steam          | 0.75                     | 90      | 0.2144            | 700-900         |
| 15     | FB        | 20             | 50           | H <sub>2</sub> /CO/steam          | 0.5                      | 90      | 0.2144            | 700-900         |
| 16     | FB        | 20             | 50           | H <sub>2</sub> /CO/steam          | 0.25                     | 90      | 0.2144            | 700-900         |
| 17     | FB        | 20             | 50           | H <sub>2</sub> /CO/steam          | CO only                  | 90      | 0.2144            | 700-900         |
| 18     | FB        | 20             | 50           | H <sub>2</sub> /CO/steam          | H <sub>2</sub> only      | 90      | 0.2144            | 700-900         |
| Blank  | TGA       | 1              | 0.01         | N <sub>2</sub>                    | n/a                      | n/a     | 0.0275            | 700-900         |
| Blank  | FB        | 20             | 50           | N <sub>2</sub>                    | n/a                      | n/a     | 0.2144            | 700-900         |
| Blank  | FB        | 20             | 50           | Steam                             | n/a                      | n/a     | 0.2144            | 700-900         |

The objective of the TGA experiments was to generate data for evaluation of different kinetic mechanisms and derive kinetic constants. TGA experiments were conducted using a Perkin-Elmer TGA-7 thermogravimetric analyzer with a TAC 7/DX control box upgrade driven by Pyris software. OTM samples (~12 mg) were preheated under a N<sub>2</sub> atmosphere (heating rate 10°C/min) to the desired temperature (700-900°C). This temperature was then maintained as a reducing gas (a mixture of CO and H<sub>2</sub> in N<sub>2</sub>) was fed at a flow rate of 30 ml/min. Pressurized gas cylinders of N<sub>2</sub>, CO and H<sub>2</sub> were used to feed the reducing gas mixture. The gases were dried using a molecular sieve moisture trap before being fed to the TGA.

TGA experimental results include the weight change of a sample as a function of time. This weight change can be directly related to the extent of the reaction conversion, since oxidized OTM (OTM-O) has a different molecular weight than reduced OTM (OTM-R). Reaction stoichiometry dictates that a weight loss of 10% corresponds to complete reaction from OTM-O to OTM-R. The extent of conversion  $[\alpha(t)]$  was calculated using the formula below:

$$\alpha(t) = \frac{m_0 - m(t)}{m_0 - m_{10\%}} \quad (\text{Equation 1})$$

Where:

$m_0$  is the initial mass,

$m(t)$  is the mass at time t, and

$m_{10\%}$  is the mass corresponding to complete conversion (10% mass loss).

The Avrami-Erofe'ev method was used to compare the kinetics of the isothermal solid-state reactions taking place in the TGA. The method is based on an equation describing nucleation and growth processes:

$$\alpha = 1 - \exp(-\beta t^m) \quad (\text{Equation 2})$$

$$\ln(-\ln(1-\alpha)) = \ln \beta + m \ln t \quad (\text{Equation 3})$$

Where:

$\alpha$  is the extent of conversion at any given time,  $t$

$\beta$  is a constant, partially depended both on nucleation frequency and rate of grain growth

$m$  is a constant associated with the geometry of the system

Plots of equation (3) yield lines with slopes  $m$  (the linear region of such plots is generally for  $\alpha$  values between 0.15 and 0.50). The value of  $m$  is indicative of the specific solid-state kinetic mechanism, as described in Table 3. Results from these tests are summarized in Section 4.1.

Table 3. Selected solid-state reaction rate equations.

|   |  |                              |
|---|--|------------------------------|
| $1 - (1 - \alpha)^{1/3} = kt$<br>$\alpha = 1 - (1 - kt)^3$        | $m = 1.07$ ; Equation for phase-boundary-controlled reaction (surface reaction) for a sphere | (Equation 4)<br>(Equation 5) |
| $-\ln(1 - \alpha) = kt$<br>$\alpha = 1 - \exp(-kt)$               | $m = 1$ ; Equation for first-order reaction  | (Equation 6)<br>(Equation 7) |
| $[-\ln(1 - \alpha)]^{1/2} = kt$<br>$\alpha = -\exp(-k^2 t^2) + 1$ | $m = 2$ ; Avrami-Erofe'ev equation for phase change model                                    | (Equation 8)<br>(Equation 9) |

The objective of the fluidized bed tests is to observe OTM reduction behavior in a system closer in configuration to the UFP process. Since it is not possible to directly measure the OTM mass change (as in TGA experiments), assumptions must be made in interpreting the data, particularly with regard to the involvement of reactions other than the OTM reduction reaction. These tests are still in progress, and results will be reported in the next quarterly report after completion of the entire matrix of fluidized bed tests.

### 3.2 BENCH-SCALE TESTING

The objectives of the bench-scale testing task are to demonstrate the technical feasibility of the UFP technology and aid in developing modeling tools and pilot plant equipment design. The bench-scale system is also intended to provide data on individual UFP reactor modes to aid in pilot plant design and testing. Bench-scale testing conducted in the third year included detailed testing of the OTM oxidation-reduction cycle.

OTM performance is related to the ability of the OTM to undergo the reduction reactions in Reactor 2 mode that in turn allow the OTM to be oxidized at Reactor 3 conditions. Experiments conducted under Reactor 3 conditions have shown that the oxidation of reduced-state OTM occurs rapidly and readily and is highly exothermic. OTM performance is most often limited by the reduction step. Initial OTM tests were conducted using coal for OTM reduction. Later tests were conducted using CO and H<sub>2</sub> as reducing agents to isolate OTM reduction from coal gasification. The complexity of the behavior observed led to the development of a designed experimental test matrix as described in the second annual report (Oct 1, 2001 – Sep 30, 2002).

The full set of test matrix experiments were completed in the third year of this program. The test conditions and results are presented in Table 4. The test conditions (independent variables) include CO and H<sub>2</sub> concentrations as well as the Gas Hourly Space Velocity (GHSV), while the % OTM reduction is the main response dependent variable. The first thirteen tests were the full test matrix, while the last two tests were optimization runs completed after analysis of the first thirteen runs. Results of these tests are discussed in Section 4.2.

Table 4. OTM test conditions for full test matrix.

| Test # | Independent Variables    |                          |                     |
|--------|--------------------------|--------------------------|---------------------|
|        | Local feed concentration |                          | GHSV                |
|        | [CO] vol. %              | [H <sub>2</sub> ] vol. % | (hr <sup>-1</sup> ) |
| 1      | 3.1                      | 12.4                     | 1798                |
| 2      | 6.4                      | 6.4                      | 1573                |
| 3      | 0                        | 7.1                      | 1718                |
| 4      | 6.1                      | 12.1                     | 1562                |
| 5      | 7.4                      | 0                        | 1665                |
| 6      | 0                        | 14.7                     | 2144                |
| 7      | 0                        | 13.2                     | 1515                |
| 8      | 5.5                      | 0                        | 3170                |
| 9      | 3.1                      | 6.2                      | 1931                |
| 10     | 3.6                      | 0                        | 1544                |
| 11     | 0.0                      | 0                        | 2443                |
| 12     | 6.0                      | 12.0                     | 2527                |
| 13     | 3.3                      | 6.6                      | 2517                |

## 4.0 RESULTS AND DISCUSSION

### 4.1 LABORATORY-SCALE TESTING RESULTS

#### 4.1.1 Coal Gasification Results

Laboratory-scale coal gasification tests were conducted in a high-temperature fluidized bed as described in Section 3.1.1. During the first 5 minutes of each test, significantly larger outlet flow rates were detected, presumably due to the early release of volatile matter. Meanwhile, hydrogen production was observed to fall to negligible amounts approximately 15 minutes after the start of all experiments. After 15 minutes, the CO<sub>2</sub> content in the outlet gases tends to increase slightly as the CAM begins to desorb CO<sub>2</sub> (caused by a shift in equilibrium since CO<sub>2</sub> concentrations have been depleted from the gas phase due to consumption of the injected coal batch). Thus, the first 5 and 15 minutes of each test were chosen as evaluation periods of significance, and the results are reported accordingly. Selected lab-scale test results are provided in Table 5 for tests conducted with a constant bed size and different coal loadings. One of the tests was conducted with an OTM bed, while three were conducted with CAM beds.

Table 5. Product gas composition and volume results obtained for tests conducted with a variety of bed:coal ratios and bed compositions.

| Test Conditions                              | Total Volume<br>(N <sub>2</sub> free basis)<br>[l] per 1g of Coal | H <sub>2</sub><br>Vol.<br>Fraction | H <sub>2</sub><br>Volume<br>[l] per 1g<br>of Coal | CO<br>Vol.<br>Fraction | CO <sub>2</sub><br>Vol.<br>Fraction | CH <sub>4</sub><br>Vol.<br>Fraction |
|--|---|------------------------------------|---|------------------------|-------------------------------------|-------------------------------------|
| <i>After 5 minutes</i>                       |   |                                    |   |                        |                                     |                                     |
| 85.7g CAM /1g of coal<br>(0.7 g coal charge) | 0.800   | 0.59                               | 0.472   | 0.20                   | 0.09                                | 0.13                                |
| 48g CAM / 1g of coal<br>(1.25g coal charge)  | 0.344   | 0.74                               | 0.255   | 0.14                   | 0.09                                | 0.02                                |
| 24g CAM / 1 g of coal<br>(2.5g coal charge)  | 0.224   | 0.63                               | 0.141   | 0.18                   | 0.14                                | 0.05                                |
| 48g OTM / 1g of coal<br>(1.25g coal charge)  | 0.232   | 0.48                               | 0.111   | 0.07                   | 0.34                                | 0.10                                |
| <i>After 15 minutes</i>                      |   |                                    |   |                        |                                     |                                     |
| 85.7g CAM /1g of coal<br>(0.7 g coal charge) | 1.070   | 0.63                               | 0.674   | 0.17                   | 0.11                                | 0.09                                |
| 48g CAM / 1g of coal<br>(1.25g coal charge)  | 0.648   | 0.70                               | 0.454   | 0.12                   | 0.15                                | 0.02                                |
| 24g CAM / 1 g of coal<br>(2.5g coal charge)  | 0.360   | 0.59                               | 0.212   | 0.17                   | 0.21                                | 0.03                                |
| 48g OTM / 1g of coal<br>(1.25g coal charge)  | 0.312   | 0.51                               | 0.159   | 0.05                   | 0.36                                | 0.08                                |

For these batch tests with the same bed size, increasing the amount of coal places an increased performance demand on the bed materials. For CAM beds, it is possible to exceed the capacity of the CAM to absorb CO<sub>2</sub>, as shown by the increasing concentrations of CO<sub>2</sub> at decreased

CAM:coal ratios. OTM beds react with CO and  $H_2$  to form reduced-state OTM, thus the CO and  $H_2$  concentrations are markedly reduced for the tests conducted with an OTM bed. These relationships are being assessed and analyzed to provide insight into the kinetics that will be used to influence the relationship between bed size and bed residence time.

Selected results from coal gasification testing are provided in Table 6 for a series of tests conducted with injection of 2.5 grams of coal and a constant bed mass (60 g). The CAM-OTM index is a measure of the relative amounts of CAM and OTM, with an index of 1 corresponding to a pure CAM bed, and an index of -1 corresponding to a pure OTM bed. As discussed

Table 6. Results from lab-scale high temperature coal gasification tests.

| Test # | Elapsed time | Bed contents (g) |     | CAM-OTM index | Gas composition (vol. fraction) |      |        |        | Volume (liters) |       |
|--------|--------------|------------------|-----|---------------|---------------------------------|------|--------|--------|-----------------|-------|
|        |              | CAM              | OTM |               | $H_2$                           | CO   | $CO_2$ | $CH_4$ | $H_2$           | Total |
| 1      | 15           | 60               | 0   | 1             | 0.59                            | 0.17 | 0.21   | 0.03   | 0.531           | 0.9   |
|        | 5            |                  |     |               | 0.63                            | 0.18 | 0.14   | 0.05   | 0.353           | 0.56  |
| 2      | 15           | 60               | 0   | 1             | 0.59                            | 0.15 | 0.23   | 0.03   | 0.472           | 0.8   |
|        | 5            |                  |     |               | 0.59                            | 0.13 | 0.13   | 0.15   | 0.330           | 0.56  |
| 3      | 15           | 55               | 5   | .83           | 0.49                            | 0.28 | 0.14   | 0.09   | 0.475           | 0.97  |
|        | 5            |                  |     |               | 0.55                            | 0.26 | 0.07   | 0.12   | 0.319           | 0.58  |
| 4      | 15           | 50               | 10  | .67           | 0.46                            | 0.23 | 0.17   | 0.14   | 0.529           | 1.15  |
|        | 5            |                  |     |               | 0.51                            | 0.19 | 0.13   | 0.17   | 0.382           | 0.75  |
| 5      | 15           | 40               | 20  | .33           | 0.53                            | 0.21 | 0.20   | 0.06   | 0.636           | 1.2   |
|        | 5            |                  |     |               | 0.47                            | 0.23 | 0.22   | 0.08   | 0.343           | 0.73  |
| 6      | 15           | 30               | 30  | 0             | 0.50                            | 0.15 | 0.26   | 0.09   | 0.545           | 1.09  |
|        | 5            |                  |     |               | 0.46                            | 0.18 | 0.23   | 0.13   | 0.280           | 0.61  |
| 7      | 15           | 0                | 60  | -1            | 0.34                            | 0.19 | 0.32   | 0.15   | 0.231           | 0.68  |
|        | 5            |                  |     |               | 0.38                            | 0.19 | 0.27   | 0.16   | 0.182           | 0.48  |

previously, Table 6 shows data from both 5 minutes and 15 minutes of elapsed testing time. Figure 2 shows the volume of product gas and the volume of  $H_2$  for each test listed in Table 6, with data from both 5 minutes and 15 minutes of testing.

Since CAM absorbs  $CO_2$ , thus removing it from the product gas, it is expected that high CAM-OTM index tests will have reduced amounts of product gas, as shown in Figure 2. This effect is balanced to some extent by increased

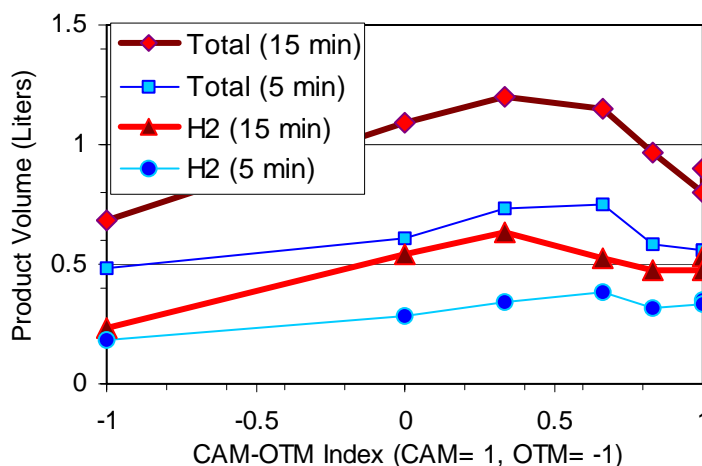


Figure 2. Lab-scale coal gasification results: product volume and  $H_2$  volume at different bed compositions.

conversion of CO to  $CO_2$  via the water-gas shift reaction. Also, as discussed above, OTM reacts with CO and  $H_2$  to form reduced-state OTM, resulting in both reduced total volume and reduced volume of  $H_2$ , as illustrated in Figure 2.

#### 4.1.2 OTM Characterization Results

TGA experiments were conducted at a range of reducing gas compositions. In each test, 90%  $N_2$  was fed, with the remaining 10% varying from all  $H_2$  to all CO and various mixtures between. Selected results are provided below.

The reaction time scale varies widely (particularly for lower temperatures) for reduction by CO and by  $H_2$ , as shown in Figures 3 and 4. Note the difference in time scales, as at 700°C, complete reduction by CO is achieved after 30 minutes, while reduction by  $H_2$  is complete after only one minute. The figures also indicate that increased temperatures reduce the time required to achieve complete conversion for any reducing gas. For example, at the expected pilot-scale operating temperature for OTM reduction ( $\sim 900^\circ\text{C}$ ), the reaction time-scale difference reduces as complete reduction by CO is achieved in about three minutes, while reduction by  $H_2$  is achieved in less than half a minute. Previous bench-scale data have shown similar behavioral trends.

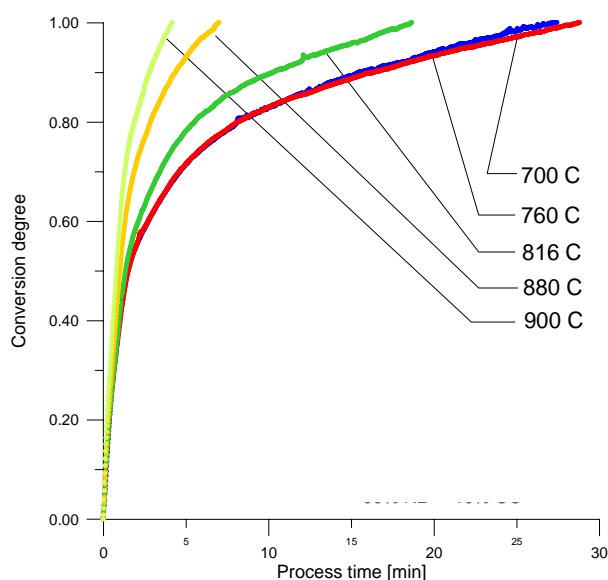


Figure 3. Conversion degree as a function of time for a 90%  $N_2$ , 10% CO mixture at a variety of temperatures.

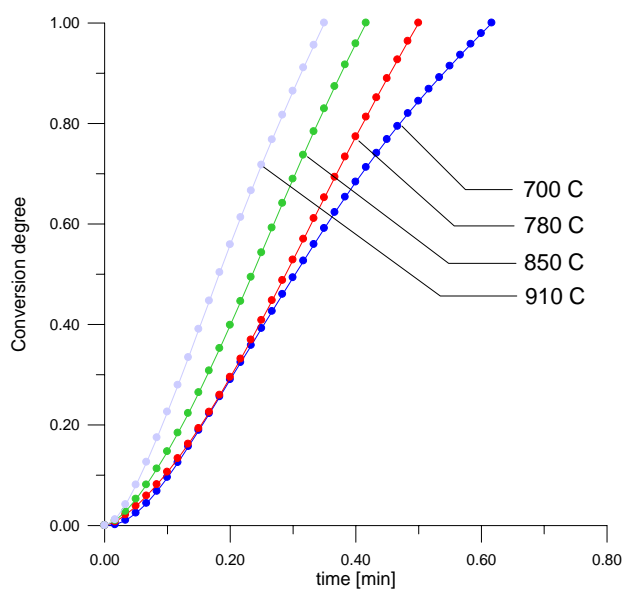


Figure 4. Conversion degree as a function of time for a 90%  $N_2$ , 10%  $H_2$  mixture at a variety of temperatures.

Preliminary kinetic analysis suggests that the initial reduction by CO (up to 50% conversion) is best described by the first-order reaction model. The observed average  $m$ -value was 0.9, close to the value of 1.0 predicted by the first-order model. For initial reduction by  $H_2$ , the average  $m$ -value was 1.7, and analysis suggests that the Avrami-Erofe'ev phase change model ( $m = 2$ ) best describes this data.

Mixtures of CO and  $H_2$  were also evaluated, and the results are shown in Figures 5 and 6. Results indicate that the Figure 5 mixture (5.7% CO, 4.3%  $H_2$ ) requires less time to achieve complete

conversion (~5 minutes) than the Figure 6  $H_2$ -dominant (2%  $CO$ , 8%  $H_2$ ) mixture (~25 minutes). These results suggest that conversion time is not linear with % $H_2$ . Similar results were reported for the bench-scale system. Kinetic analysis indicated that the initial reduction behavior of both mixtures was best described by the Avrami-Erofe'ev phase change model. The Figure 5 mixture had an average m-value of 1.6, while the  $H_2$ -dominant mixture (Figure 6) had an average m-value of 1.15. Additional analysis of data to confirm stated observations is continuing.

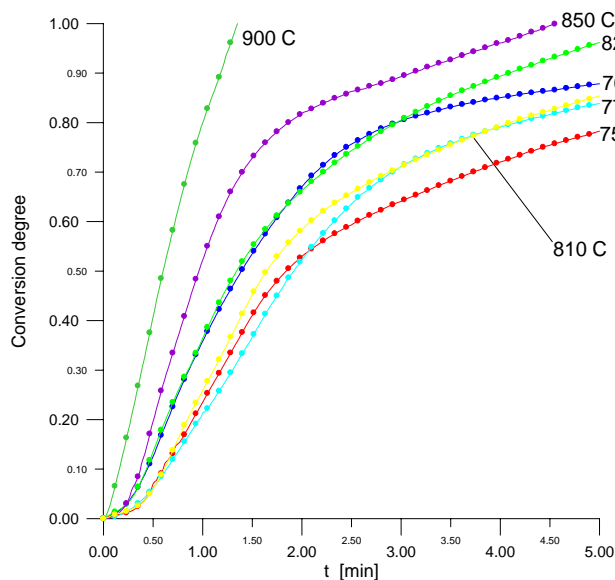


Figure 5. Conversion degree as a function of time for a 90%  $N_2$ , 5.7%  $CO$ , 4.3%  $H_2$  mixture at a variety of temperatures.

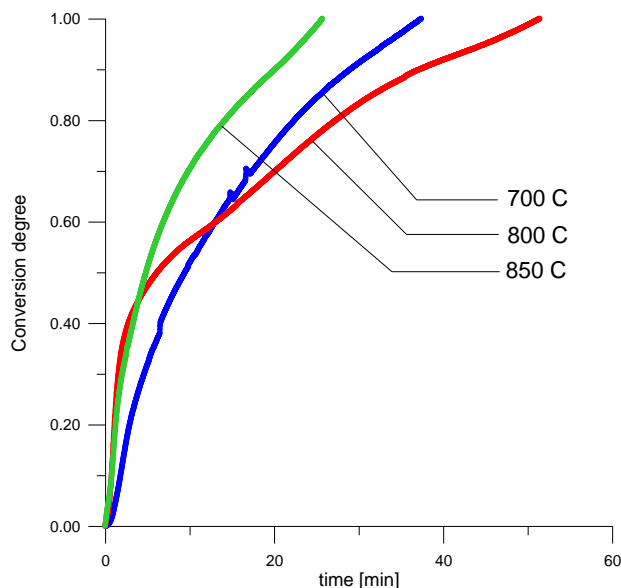


Figure 6. Conversion degree as a function of time for a 90%  $N_2$ , 2%  $CO$ , 8%  $H_2$  mixture at a variety of temperatures.

Using k-values from the derived kinetic expressions along with temperatures, reaction data were used to derive preliminary activation energy values. Due to some perturbations associated with low temperatures ( $<780^\circ C$ ), activation energies were derived using only data from temperatures between  $780$ - $900^\circ C$ , as recommended by Tokuda (1979).

## 4.2 BENCH-SCALE TESTING RESULTS

After completion of the test matrix described in Section 3.2, an initial transfer function was developed and used to identify operating conditions predicted to provide peak OTM reduction. Two additional optimization tests were conducted at the conditions predicted to provide high OTM reduction. The results in Table 7 show that the %OTM reduction achieved in these tests exceeded the performance of all previous test runs and validated predictions of the initial transfer function. An optimized transfer function was then derived based on all fifteen tests based on a surface fit and making use of second-order interactions. This transfer function is provided below as Equation 10.

$$X_{OTM} = 44.7 + 1.6[CO] - 0.93[H_2] - 0.033GHSV - 0.13[CO][H_2] + 8.8 \times 10^{-4}[H_2]GHSV - 0.17[CO]^2 - 0.013[H_2]^2 + 6.9 \times 10^{-6}GHSV^2 \quad (\text{Equation 10})$$

Table 7. OTM test conditions and results for full test matrix.

| Test # | Independent Variables    |                          |                     | Response      |
|--------|--------------------------|--------------------------|---------------------|---------------|
|        | Local feed concentration |                          | GHSV                | OTM reduction |
|        | [CO] vol. %              | [H <sub>2</sub> ] vol. % | (hr <sup>-1</sup> ) | (%)           |
| 1      | 3.1                      | 12.4                     | 1798                | 10.6          |
| 2      | 6.4                      | 6.4                      | 1573                | 9.4           |
| 3      | 0                        | 7.1                      | 1718                | 10.8          |
| 4      | 6.1                      | 12.1                     | 1562                | 6.9           |
| 5      | 7.4                      | 0                        | 1665                | 10.2          |
| 6      | 0                        | 14.7                     | 2144                | 15.4          |
| 7      | 0                        | 13.2                     | 1515                | 12.8          |
| 8      | 5.5                      | 0                        | 3170                | 11.1          |
| 9      | 3.1                      | 6.2                      | 1931                | 10.9          |
| 10     | 3.6                      | 0                        | 1544                | 12.9          |
| 11     | 0.0                      | 0                        | 2443                | 4.0           |
| 12     | 6.0                      | 12.0                     | 2527                | 11.5          |
| 13     | 3.3                      | 6.6                      | 2517                | 12.7          |
| Opt-1  | 0                        | 13.1                     | 2611                | 19.0          |
| Opt-2  | 0                        | 14.0                     | 2452                | 20.0          |

Where:

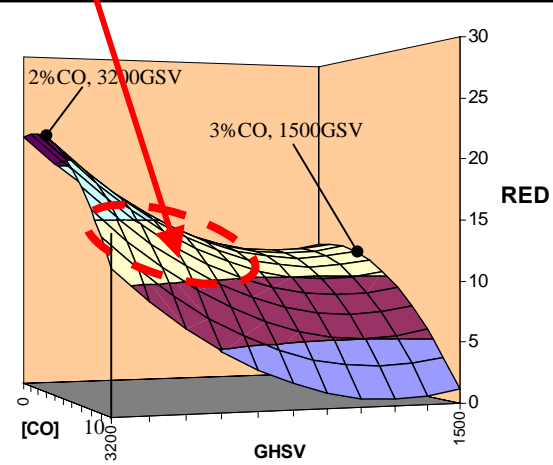
- $X_{OTM}$  = fraction of OTM reduced (wt%)
- [CO] = concentration of CO at 900°C and 300 psi (0 – 7.4 vol. %)
- [H<sub>2</sub>] = concentration of H<sub>2</sub> at 900°C and 300 psi (0 – 14.7 vol. %)
- GHSV = gas hourly space velocity, volumetric steam flow/volume of bed (1500 – 3200)

The 15-test transfer function was used to calculate predicted performance for the actual test conditions, and these predictions were compared to the actual experimental results. The results of this comparison are shown in Table 8, and show excellent agreement. A three-dimensional plot of the effects of CO concentration and GHSV on OTM reduction at 10% H<sub>2</sub> concentrations is shown in Figure 7. The region of expected pilot-scale operation is shown, and is expected to result in reduction of up to 20% of the OTM present in the bed.

Table 8. Comparison of transfer function predictions with actual experimental data.

| Predicted Results |        |      |       |        |
|-------------------|--------|------|-------|--------|
| Point             | Actual | Pred | Resid | %Error |
| 1                 | 10.6   | 11.1 | -0.50 | 4.66   |
| 2                 | 9.4    | 9.2  | 0.16  | -1.66  |
| 3                 | 10.8   | 11.0 | -0.20 | 1.89   |
| 4                 | 6.9    | 6.6  | 0.37  | -5.31  |
| 5                 | 10.2   | 10.3 | -0.15 | 1.50   |
| 6                 | 15.4   | 15.8 | -0.39 | 2.52   |
| 7                 | 12.8   | 12.8 | -0.02 | 0.12   |
| 8                 | 11.1   | 11.2 | -0.02 | 0.15   |
| 9                 | 10.9   | 10.7 | 0.13  | -1.20  |
| 10                | 12.9   | 12.8 | 0.06  | -0.44  |
| 11                | 4.0    | 4.0  | 0.03  | -0.66  |
| 12                | 11.5   | 11.7 | -0.30 | 2.60   |
| 13                | 12.7   | 12.5 | 0.21  | -1.66  |
| 14                | 19.0   | 19.8 | -0.77 | 4.04   |
| 15                | 20.0   | 18.6 | 1.39  | -6.96  |
|                   | Actual | Pred | Resid | %Error |
| Minimum           | 4.0    | 4.0  | -0.77 | -6.96  |
| Maximum           | 20.0   | 19.8 | 1.39  | 4.66   |
| Average           | 11.9   | 11.9 | 0.00  | -0.03  |
| Std Dev           | 4.1    | 4.0  | 0.48  | 3.18   |

**Pilot system expected operating region:**  
 [CO]: 1 – 5 vol.%  
 GHSV: 2300 – 3200  
 Reduction: 12 – 20wt%


 Figure 7. Transfer function predictions of OTM reduction as a function of CO concentration and GHSV at 10% H<sub>2</sub> concentration.

### **4.3 ENGINEERING AND MODELING STUDIES**

The objectives of the Process Modeling effort are to develop models for the UFP technology, validate them using experimental data, and apply the models to assist in the design and operation of the pilot-scale system. In addition, process models will be used to make meaningful comparisons of the performance of the UFP technology relative to competing technologies.

UFP process modeling was performed using Aspen Plus version 11.1. Aspen Plus (Aspen Technology, Inc.) is engineering software that can perform process analysis for various unit operations (including reactions, separations, drying, etc.) and process design calculations for heat exchangers, pumps and turbines. Aspen Plus can also handle steady-state processes involving solids such as coal. Some of the solids processing applications that have been modeled with Aspen Plus include:

- The Bayer process
- Cement kilns
- Coal gasification
- Hazardous waste incineration
- Iron ore reduction
- Zinc smelting/roasting

These capabilities make Aspen Plus a suitable process analysis tool for the UFP technology, which includes chemical processes involving solids such as coal, CO<sub>2</sub>-absorbing material (CAM), and oxygen transfer material (OTM).

Modeling work conducted this year has focused on development of an ASPEN process model of the pilot-scale system to assist in determining initial operating conditions for system shakedown, and development of an integrated UFP model to address integration of the UFP technology with other Vision 21 modules (Task 8) and compare it to competing IGCC systems.

#### **4.3.1 Pilot-Scale System Process Modeling**

An ASPEN process model of the pilot-scale system was developed to help identify initial operating conditions. Key process variables were initially identified during a series of six-sigma workout sessions. Initial modeling efforts were aimed at using sensitivity analysis to reduce the number of variables of interest. More recent efforts have identified key variables of interest for pilot-scale operating conditions. These input parameters are identified in Table 9.

The ASPEN-based model developed for the UFP pilot-scale system features three reactors interconnected with solids transfer ducts. Coal and steam are fed into the first reactor, steam is fed into the second reactor, and air fed into the third reactor. Auxiliary steam is fed into the solids transfer ducts to entrain and transport bed materials between reactors. Unit operations unique to ASPEN include the use of a virtual coal decomposer (because ASPEN does not recognize coal as a component), a separator unit (to separate the solids and the gases exiting each reactor), a mixer (to add steam to the solids being transferred between reactors), and a solids splitter (to divide the solids stream exiting Reactor 2 into R1- and R3-bound components according to the specified split ratio). The process flow diagram used for the ASPEN simulation is shown in Figure 8.

Table 9. Input parameters for UFP pilot-scale simulation.

| Critical Operating Conditions | Fixed                                | Range           | Note  |
|-------------------------------|--------------------------------------|-----------------|---|
| Coal feed rate (lb/hr)        |                                      | Up to 100 lb/hr | Limited by reactor design specs to operate in bubbling bed regime |
| Coal conversion               |                                      | 0-1             |   |
| Initial OTM:CAM ratios        |                                      | 0-1             |   |
| Solid split ratio in R2       | 1 part to R1,<br>2 parts to R3       |                 | Limited by solids transfer system capabilities                    |
| Solids recirculation rate     | ~ 450 kg/hr exiting R2               |                 |   |
| Reactor temperatures          | ~ 750, 900,<br>1150 °C, respectively |                 | From bench-scale experiments and material limits                  |
| % water in slurry             | 50%                                  |                 | Initial shakedown tests   |
| Fluidized bed feed flow       | 2 x minimum fluidization             |                 | Minimum limit to maintain bubbling bed regime                     |

In order to obtain desirable performance from the system, each reactor was optimized individually. The three key input variables for the simulation included the coal feed rate to R1, the coal conversion in R1 and the initial OTM bed fraction. The coal feed rate was varied between 20-65 lb/hr, and the coal conversion and OTM bed fraction were varied between 0 and 1. For the initial shakedown conditions selected, the best agreement between the optimal conditions of the three reactors was obtained at a coal feed rate of approximately 25 lb/hr. Tecplot v.10 software was used to obtain contour plots that show the relationship between the input variables and the performance variables of interest. Figure 9 shows reactor temperatures as a function of coal conversion and initial OTM bed fraction at a coal feed rate of 25 lb/hr. Since

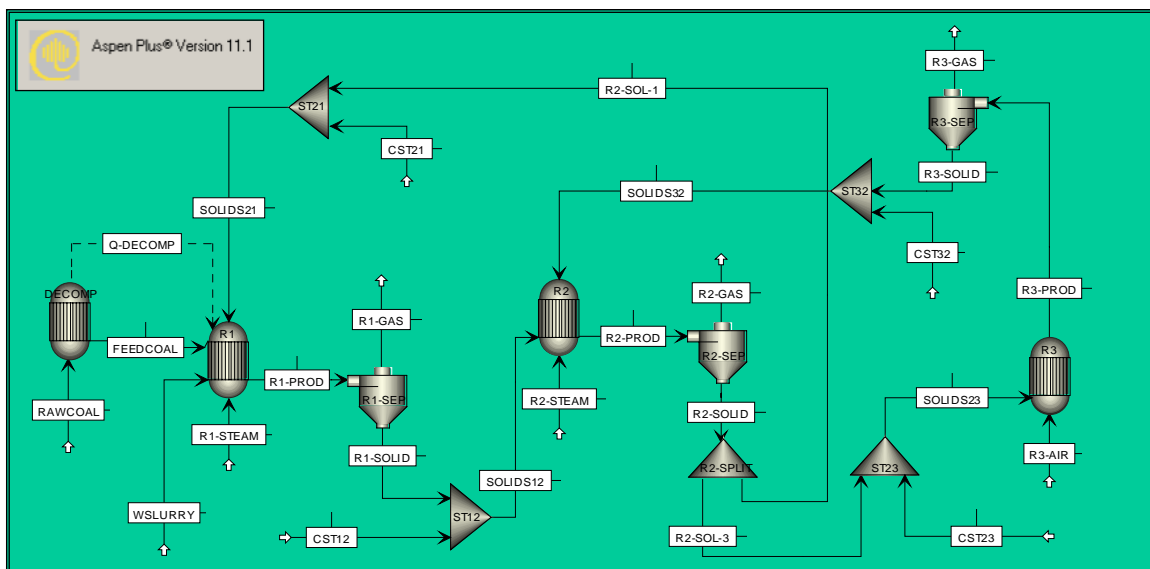


Figure 8. ASPEN simulation process flow diagram for UFP pilot-scale system.

the maximum feed temperature for each of the reactors is 900-950°C (a limitation of the coils carrying steam through the superheater), all regions with temperatures that exceed 950°C can be ruled out from consideration for initial tests (If desired, the coil type can be changed later to a grade that withstands temperatures  $>950^\circ C$ ). The region of operating conditions that satisfies this requirement for all three reactors is shown in Figure 9 as a dotted box for coal conversion between 0.4 and 0.6 and initial OTM fraction between 0.5 and 0.6.

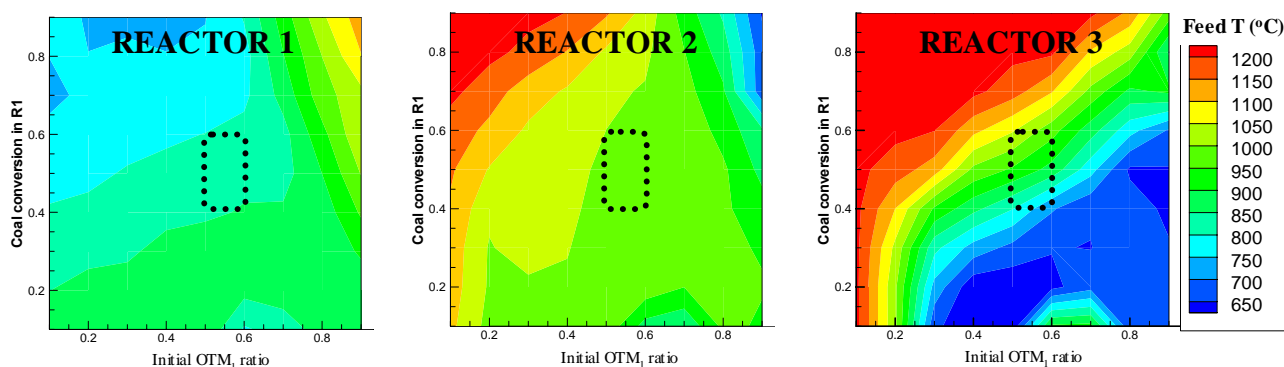


Figure 9. Contour plots that represent the temperature as a function of coal conversion and initial OTM bed fraction ( $OTM_1$ ) at a coal feed rate of 25 lb/hr.

Figure 10 shows the impact of coal conversion and initial OTM fraction on four key performance indicators ( $H_2$  product concentration in R1, fraction of C in coal separated as  $CO_2$  in R2,  $H_2$  concentration in R2, and  $CO_2$  concentration in R3) at a coal feed rate of 25 lb/hr. The model predicts that in the range of operating conditions specified (25 lb/hr coal feed, initial OTM fraction: 0.5-0.6 and R1 coal conversion: 0.4-0.6), the pilot-scale system will be able to achieve:

- $H_2$  concentration in R1  $>85\%$
- Percentage of C in coal separated as  $CO_2$  in R2  $>75\%$
- $H_2$  concentration in R2: 30-35%
- $CO_2$  concentration in R3  $<3\%$

The performance objectives of the pilot-scale system are to maximize  $H_2$  production in R1, minimize  $H_2$  slip in R2, maximize  $CO_2$  release in R2 and minimize  $CO_2$  slip in R3. These results represent the limiting case of chemical equilibrium. The process may also be limited by kinetics, and future-modeling efforts will consider this other limiting case. The  $H_2$  slip in R2 seems to be a result of the small scale of the system. Analysis of larger plants has shown that large plants have negligible  $H_2$  slip in R2 due to their high solids recirculation rates, as  $H_2$  is consumed by reduction of the OTM. This issue will be investigated further in future modeling efforts.

Pilot-scale modeling results provide insight into the behavior of the pilot-scale system and suggest the ability of the UFP pilot-scale system to meet program objectives.

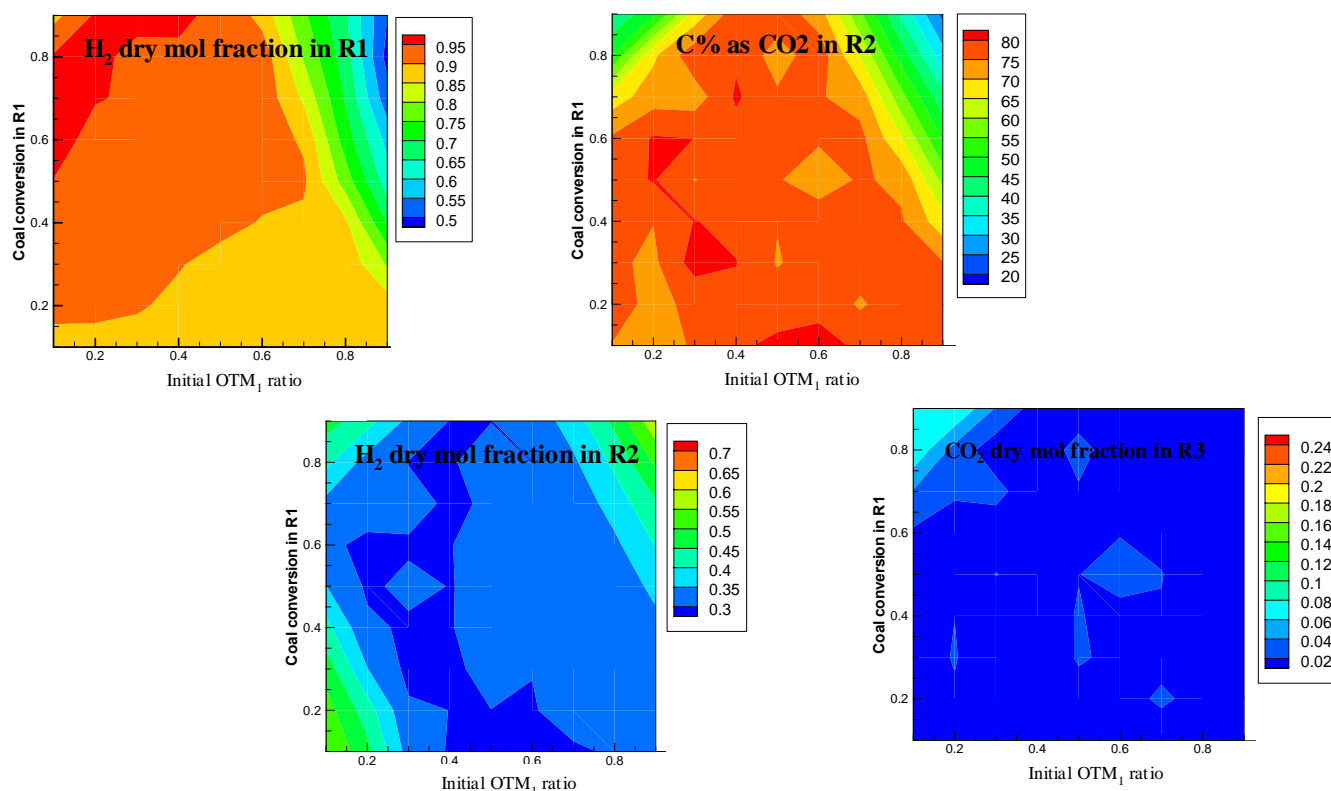


Figure 10. The impact of initial OTM fraction and coal conversion on four key performance indicators ( $H_2$  product concentration in R1, fraction of C in coal separated as  $CO_2$  in R2,  $H_2$  concentration in R2, and  $CO_2$  concentration in R3) at a coal feed rate of 25 lb/hr.

#### 4.3.2 UFP Integrated System Process Modeling / Comparison with IGCC (Task 8)

A process model was also developed for a full-scale UFP system integrated with a combined cycle plant. The process flow diagram was constructed in Aspen Plus as shown in Figure 11. The first reactor produces  $H_2$ -rich fuel, the second reactor produces a  $CO_2$ -rich stream at the process pressure (30 atm) and the third reactor produces vitiated air at high temperature and pressure.

The product of the first reactor is sent to a  $H_2$  separation device such as a pressure swing adsorber (PSA) after gas clean up and heat recovery. The product of the second reactor is sent to a  $CO_2$  compressor to be further compressed to sequestration-ready condition after going through a heat recovery unit and condenser. The product of the third reactor is sent to a gas turbine and a heat recovery steam generator (HRSG) unit. Figure 12 shows the process flow diagram for the entire steam cycle including the HRSG and steam turbines. The steam cycle section was provided by the US DOE (NETL office), and makes use of realistic assumptions. Key assumptions of the model are listed in Table 10. The process model for the UFP process and the combined cycle plant follows DOE process modeling guidelines.



Annual Technical Progress Report 2003, October 2003

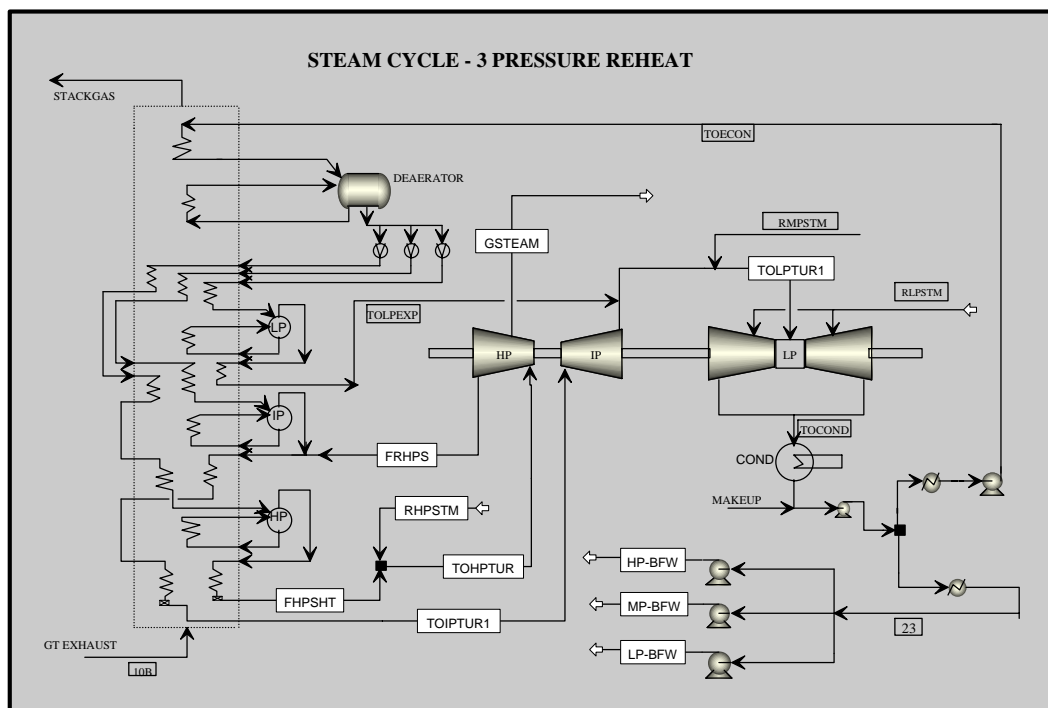


Figure 12. Process flow diagram for the 3-pressure reheat steam cycle.

Table 10. Major process modeling assumptions for the full-scale UFP integrated with combined cycle plant.

|    |   |
|----|---|
| 1  | Three main reactors (gasifier, CO <sub>2</sub> separator and oxidizer) thermodynamically limited at steady state (Gibbs reactors)   |
| 2  | Maximum temperature of the OTM limited to 1275°C at steady state  |
| 3  | Maximum heat exchanger metal temperature limited to 650°C   |
| 4  | Process conducted at 30 atm pressure  |
| 5  | Simulated gas turbine: (LM 6000 SPT) with 3-stage expansion and cooling air   |
| 6  | 3-pressure reheat steam cycle with high, intermediate and low pressure steam turbines <ul style="list-style-type: none"> <li>○ Steam generated at: 1800, 500, 300, 42 and 17 psi</li> <li>○ Internal pinch point: 15°C</li> </ul>   |
| 7  | Mechanical and auxiliary losses (in compressors, turbines, control systems etc.) <ul style="list-style-type: none"> <li>○ Mechanical losses in ST Generator: 1.5%</li> <li>○ Mechanical and generator losses in GT Generator: 2.5%</li> <li>○ Auxiliary losses: 2%</li> </ul> |
| 8  | Stack gas temperature: 100°C  |
| 9  | CO <sub>2</sub> stream compressed to 2100 psi (sequestration-ready pressure)  |
| 10 | Coal type: Illinois #6 Old Ben #26 Mine (HHV 11,666 Btu/lb)   |

#### *UFP efficiency estimates and comparison with IGCC process efficiency*

The efficiency of the process configuration was estimated as follows based on the results obtained using the Aspen Plus simulations.

$$\text{Net Efficiency, \%} = \frac{\text{HHV of H}_2 \text{ produced (MW)} + \text{Net electricity (MW)}}{\text{HHV of coal fed (MW)}} \times 100 \% \quad (\text{Equation 11})$$

The equivalent electrical efficiency was obtained by assuming that the H<sub>2</sub> generated in the process is utilized in a solid oxide fuel cell/combined cycle combo with 75% overall conversion efficiency, as defined in Equation 12.

$$\text{Equivalent electrical efficiency \%} = \frac{0.75 * \text{HHV of H}_2 \text{ produced (MW)} + \text{Net electricity (MW)}}{\text{HHV of coal fed (MW)}} \times 100 \% \quad (\text{Equation 12})$$

The process efficiency of the UFP system was compared to an IGCC process. Figure 13 shows the simplified process flow diagrams for (A) a typical IGCC system with CO<sub>2</sub> separation and (B) a UFP-combined cycle system. The process model assumptions were identical for both systems to allow direct comparison of the results. The three UFP reactors were replaced with a gasifier, a CO<sub>2</sub> separator and an air separation unit (ASU) for the IGCC process simulation.

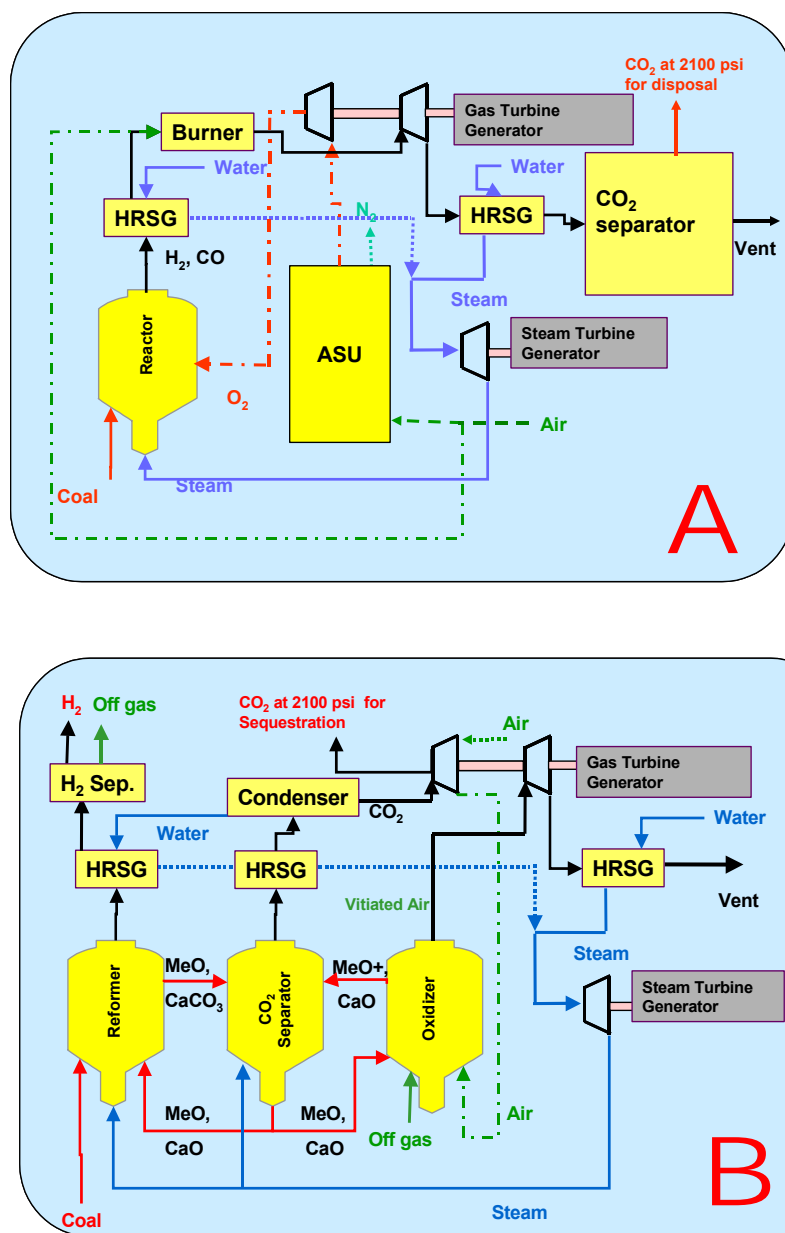


Figure 13. Process flow diagrams for (A) Typical IGCC process with CO<sub>2</sub> separation and (B) UFP process integrated with the combined cycle plant

Table 11 shows the relative comparison between the UFP process and the IGCC process efficiencies. Both the technologies were compared at 85% CO<sub>2</sub> separation. The H<sub>2</sub> to electricity ratio used for both processes was 0.4.

The process analysis shows that the UFP technology is approximately 6% more efficient as compared to the IGCC process with conventional CO<sub>2</sub> separation. With further optimization of the UFP operating parameters, including steam usage, reactor temperatures, space velocity and

solids compositions/ratios, the UFP efficiency could be up to 10% higher than the typical IGCC process with CO<sub>2</sub> removal.

Table 11. Comparison of the efficiencies for the IGCC process and the UFP technology.

| <b>Difference in energy utilization</b>   | <b><math>\Delta = \text{UFP} - \text{IGCCw/CO}_2</math></b> |
|---|---|
| Air Separation, % of coal HHV   | 3%  |
| H <sub>2</sub> HHV, % of coal HHV   | 3%  |
| Gas Turbines Net, % of coal HHV   | -0.2%   |
| Steam Turbines Net, % of coal HHV   | -2%   |
| CO <sub>2</sub> Compression, % of coal HHV                                      | 2%  |
| Auxiliary Losses, % of coal HHV   | 0%  |
| <b>Net H<sub>2</sub> and Electricity Efficiency Difference</b>                  | <b>6%</b>   |
| <b>Expected efficiency difference with optimization and advanced technology</b> | <b>~10%</b>   |

The overall advantages of the UFP system over the IGCC process are listed below:

1. The UFP technology does not require the use of an Air Separation Unit (ASU).
2. The UFP technology does not require the use of an additional CO<sub>2</sub> separation unit, due to its inherent CO<sub>2</sub> separation.
3. The UFP technology uses the higher-efficiency Bryton-Rankine cycle, while the IGCC process uses the less-efficient Rankine cycle as well as the Bryton-Rankine cycle.
4. In the UFP process CO<sub>2</sub> is removed at the process pressure (30 atm), while in the IGCC process CO<sub>2</sub> is separated at near atmospheric pressure.

As a result of the above advantages, and consistent with preliminary modeling results, UFP efficiencies are estimated to be higher than IGCC system efficiencies as shown in Table 11. This improved process efficiency also leads to competitive costs of electricity and H<sub>2</sub> for the UFP technology relative to the IGCC process.

Future process modeling and analysis work will include the following:

- Optimization of UFP process efficiency based on the modeling and experimental results.
- Comparison of the efficiency of the IGCC and UFP technologies at various H<sub>2</sub> to electricity co-production ratios to identify the optimum operating conditions.
- Development of a robust CO<sub>2</sub> separation unit simulation using a chemical solvent
- Developing a dynamic model to analyze the start-up of the UFP technology to aid in development of an UFP technology control strategy.

## 4.4 PILOT PLANT DESIGN & ASSEMBLY

The design of the pilot plant was reviewed and updated in the third program year. Although delays in obtaining a South Coast AQMD permit to “construct and operate” have prevented the system from being assembled as a single unit, work has progressed on individual components. In addition, all equipment and instrumentation have been procured and are currently on site awaiting assembly once the permit is granted. A summary of key activities and accomplishments is provided below.

### 4.4.1 Safety Analysis

A detailed safety and hazard analysis has been conducted for the pilot plant, following design for Six Sigma (DFSS) methodologies. A failure mode and effects diagram was developed to identify potential hazards, their causes and effects, as well as possible mitigation steps that could be taken to minimize their likelihood or severity. In addition, the safety and emergency shutdown system has been designed, including the shutdown state of every piece of energized equipment and a detailed understanding of the path the venting gases will take. The criteria for different levels of shutdown and alarms have also been quantified. Standard operating procedures are currently being written and reviewed for every major piece of equipment, including decision trees for various types of system malfunctions.

### 4.4.2 Reactor Design and Construction

A detailed design review was conducted to ensure that the reactors meet ASME code standards. The reactors were fabricated in the GEGR machine shop in Irvine and subjected to hydrostatic testing at 900 psi and ambient temperature. After 48 hours of exposure, minimal pressure loss was identified and inspection showed no loss of integrity in the reactor or welds. All the welded ports on all three vessels passed the test. Figure 14 is a photo of Reactor 2 undergoing hydrostatic testing.



Figure 15. Reactor 1 shell with two-cast refractory layers.

After verification of the integrity of the reactor shell, the three reactors were cast with two layers of refractory, as shown in Figure 15. First, a 2 1/8" layer of Kaolite 2300-LI was cast, followed by 1 3/8" of KaoTAB95. The solids transfer ducts were also cast with the same

refractory layers. For each layer cast, forms were designed to provide the appropriate refractory thickness, and a jig was used to hold the forms in place with the reactors standing vertically. A combination of mixing and vibration was used to ensure that the refractory material was tightly packed. Each refractory layer was allowed to set for 24 hours before removal of the jig and forms. This process was then repeated for the second refractory layer.



Figure 14. Hydrostatic test of Reactor 2.

The refractory will be cured when the complete system is assembled and the preheating system is installed. Details of the refractory design and associated reactor temperature profiles were provided in Quarterly Technical Progress Report No. 10, April 2003.

The distributor plates that will be used in the pilot-scale system were designed and tested. The same design will be used for the distributor plate in each reactor. Working closely with GE EER's machine shop, the innovative approach includes the use of  $\frac{1}{2}$ " hex bolts with a  $\frac{1}{4}$ " hole drilled from the bottom up to the bolt head, where three  $\frac{1}{16}$ " nozzle holes were drilled completely through the bolt head to produce six nozzles. The orientation of the bolts allows for staggered nozzle flows to enhance fluidization. The distributor plate was designed to operate at temperatures up to  $1000^\circ C$  and provide 10psi of differential pressure. A support sleeve is used to locate the distributor plate in the correct region and prevent the fluidization gas from bypassing the distributor plate. The distributor plate design is shown in Figure 16, including a close-up view of the bolts used as nozzles.

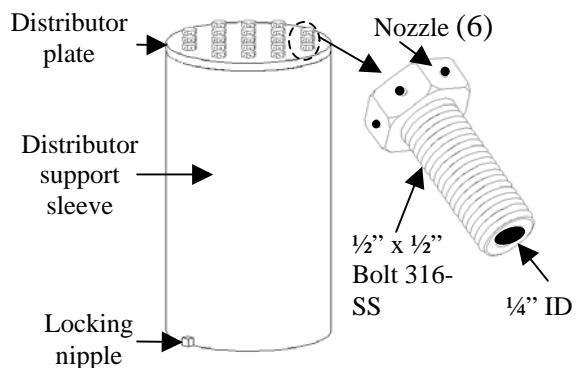


Figure 16. Pilot-scale distributor plate design with detail of nozzle bolts.



Figure 17. Photo of three pilot-scale reactors mounted on stand.

The three reactors are connected by a series of flanged solids transfer ducts. Each of Reactors 1 and 3 have two solids transfer ducts, while Reactor 2 has four solids transfer ducts. The appropriate alignment of the reactors is essential to their leak-free assembly. A stand was manufactured to provide the appropriate reactor spacing and alignment. The stand is also designed to support the weight of the filled, flanged reactors. The design of the stand required that pairs of gussets be welded to each reactor. These gussets allow the reactors to be supported from the middle of the reactors, allowing for thermal expansion while providing access to the reactors from below. Figure 17 is a photo of the three reactors mounted on the stand next to the machine shop with assembly of the solids transfer ducts.

#### 4.4.3 Coal, Steam and Air Feeding Systems

Systems were developed to allow coal, steam and air to be fed to the pilot-scale reactors. The coal will be fed as coal-water slurry, steam will be generated in a boiler and superheater, then passed through a second-stage superheater to provide the needed reactor inlet temperatures. Air will be conditioned and compressed so that it can be fed at high pressure.

A Seepex progressive cavity pump (rated for 0.2 gpm at 300psi) has been tested for its ability to pump coal-water slurry into a high-pressure vessel. Shakedown testing of the pump system has led to a reconfiguration of the pressure relief to incorporate a pressure switch to shut down the pump rather than relieving pressure (which was identified as a potential hazard in the safety review.) Initial testing of the pumping system demonstrated the ability of the pump to deliver slurry into a pressure vessel maintained at 300psi. In addition, a stirring system was used to minimize settling in the tank feeding the pump.

Hercules Boiler of Los Angeles, CA has constructed a 900 lb/hr boiler and superheater. The boiler is currently being tested at the manufacturer's site and will be delivered fully instrumented and ready for use. Due to temperature limitations of steam metering equipment, it is necessary to provide additional superheating to each steam feed line after the flow rate has been controlled to its desired set point. This is accomplished through the use of five second-stage superheaters. The second-stage superheaters consist of a 46 kW electric furnace that contains a metal coil, as shown in Figure 18. The length of the coil and the size of the furnace were specified based on detailed heat transfer analysis to allow the heating of a 400°C inlet stream to a temperature of 900°C, the required feed temperature for some reactors.

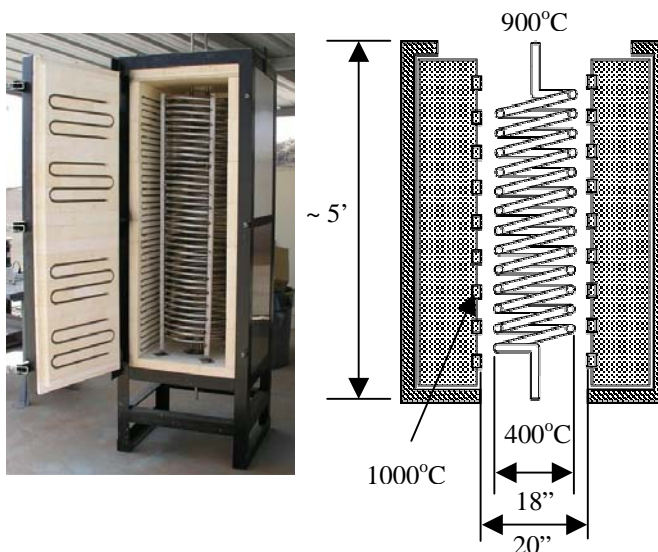


Figure 18. Photo and schematic diagram of second-stage superheater: electric furnace and heating coil.



Figure 19. High-pressure air feeding system: high pressure and low-pressure receiver tanks.

The air system makes use of a low-pressure air compressor and a high-pressure booster, along with two 240-gallon receiver vessels to provide uninterrupted flow of high-pressure air to the system. A Davey 50-BAQ screw-type air compressor is used to charge the low-pressure receiver vessel with 120psi air. This air is then fed to the Kaeser N 501-G air booster, which has a capacity of 115cfm @450psi. The high-pressure receiver vessel is maintained at 500psi, and allows steady flow of high-pressure air to the system while the booster cycles on and off. Figure 19 is a photo of the air feeding system. The Davey compressor is located behind the two receiver vessels, and the Kaeser air booster is in the foreground. A dryer is used to remove moisture from the air after the Davey compressor.

#### 4.4.4 Solids Transfer System

The transfer of solid bed materials between reactors is a critical part of the UFP technology, as it serves to transfer heat and regenerated reactants between reactors. As described in the second annual report (Oct 2002), a full-size pilot-scale cold flow model was constructed to simulate the action of the solids transfer ducts and aid in the development of the solids transfer mechanism for the pilot-scale system. This cold flow model, shown in Figure 20, has provided valuable data regarding the effectiveness of different configurations. Figure 21 is a cutaway view of the final design of Reactor 2, showing the location of the two solids transfer ducts that transport bed materials out of Reactor 1 and Reactor 3, respectively, into Reactor 2. The ducts for transport of bed materials out of Reactor 2 into Reactor 1 and Reactor 2 are not shown in the cutaway view but can be seen in the inset picture.



Figure 20. Cold flow model: 3 circulating fluidized beds.

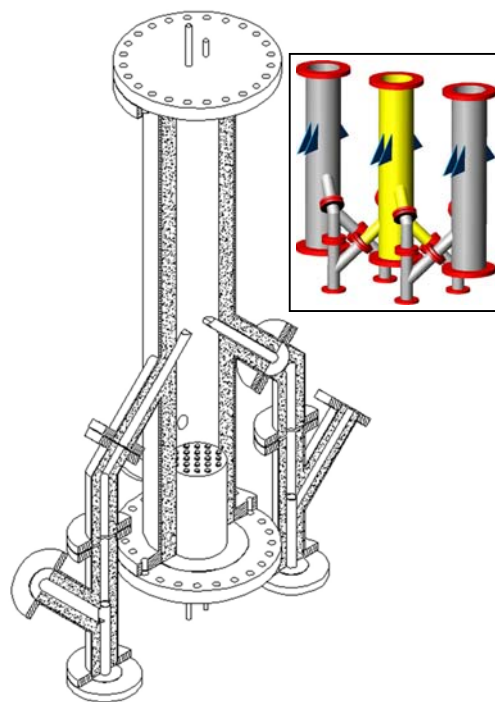


Figure 21. Cutaway view of Reactor 2 (see 3-reactor inset) showing solids transfer ducts and reactor internals.

#### 4.4.5 Auxiliary Systems

**Emissions Control System.** A system was designed to control potential emissions of  $CO$ ,  $H_2$  and unburned hydrocarbons and sulfur from the UFP operation. The system includes an afterburner, which is used to completely oxidize gasification intermediates and the  $H_2$  product, as well as a scrubber and quench for removal of sulfur compounds. The design of the quench was completed to allow cooling of the product gas from the afterburner before the gas is fed to the scrubber, which is very temperature sensitive. Figure 22 is a photo of the integrated afterburner, quench and scrubber emission control system.

The final length of the afterburner was set to allow a residence time of 1 second, in order to ensure complete destruction of CO and any organic hydrocarbons. The scrubber was located after the afterburner to ensure that all sulfur compounds are in an oxidized state, in accordance with the design specifications for the type of scrubber selected.

#### 4.4.6 UFP Pilot Plant Layout

A detailed three-dimensional model of the UFP pilot plant has been developed using AutoCAD to aid in system assembly. This model makes use of the actual dimensions of system components, and has been used to assess clearances and accessibility. This information will be of key importance in assembling the pilot plant.

The framework for the reactors and the scaffolding for the system have been designed and manufactured and are awaiting permit approval for assembly. Figure 23 is to-scale drawing showing the layout of the pilot-scale system in relation to the control room and bench-scale system.



Figure 22. Emissions control system: afterburner, quench, and scrubber in series.

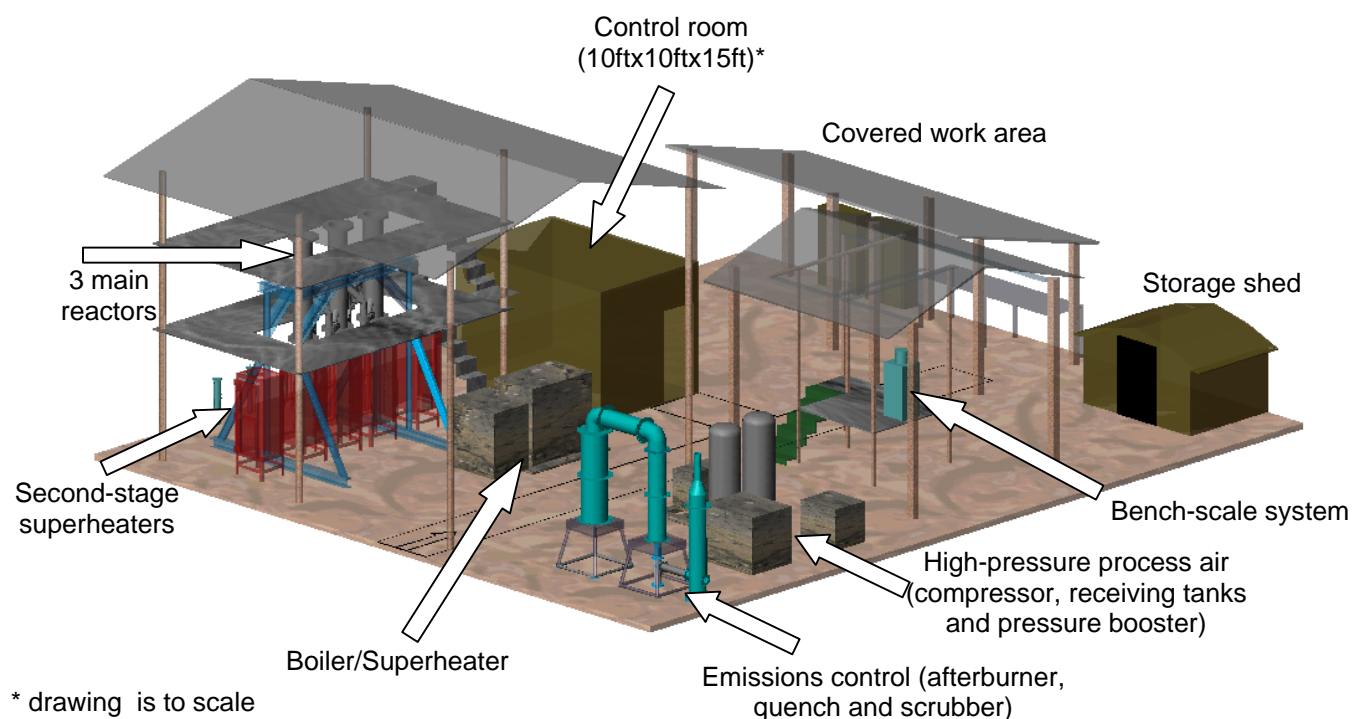


Figure 23. Layout of pilot-scale system.

#### **4.4.7 Control, Monitoring and Analysis Systems**

The control of the pilot-scale system will be conducted via using National Instruments LabVIEW software and hardware, including virtual PID controllers. A system-specific program is currently under development, and will include an interactive user interface to allow the operator to change set points for controllers and the status of valves individually and as part of an integrated test sequence.

Monitoring of the system will be conducted with a variety of pressure, temperature, concentration and flow transmitters that interface with the LabVIEW program. Figure 24 is a process and instrumentation diagram (P&ID) for the pilot-scale system showing the location of these transmitters as well as other gauges, equipment and control, and manual valves. Analysis of the concentrations of the product gas will be conducted with both continuous emissions monitors (CEMS) and a micro gas chromatograph (GC). Dedicated CEMS will be used for the product gases from each reactor, while the GC will be used to periodically assess the composition of individual reactor product streams as needed, but primarily for measurement of H<sub>2</sub> in Reactor 1 and Reactor 2. All measurements will be recorded for later analysis and reporting.

In addition to analysis of product gases, a method was developed to allow sampling of bed solids while the pilot-scale system is operating. Removal of solids from a high-temperature, high-pressure system is admittedly complex, but it will provide valuable information on the state of the bed materials in each reactor. After detailed analysis, the solids transfer ducts were identified as the best location to obtain solids samples. These bed samples can be removed and sent for analysis, providing information on the effectiveness of the OTM and CAM bed materials and the extent of their utilization in the process.

The pilot-scale system has been designed to allow the control of operating parameters within design limits and the monitoring and recording of key process variables and performance indicators. This information will aid in quantifying the performance of the system and assessing the ability of the UFP process to meet DOE objectives.

# Fuel-Flexible Gasification-Combustion Technology for Production of $H_2$ and Sequestration-Ready $CO_2$

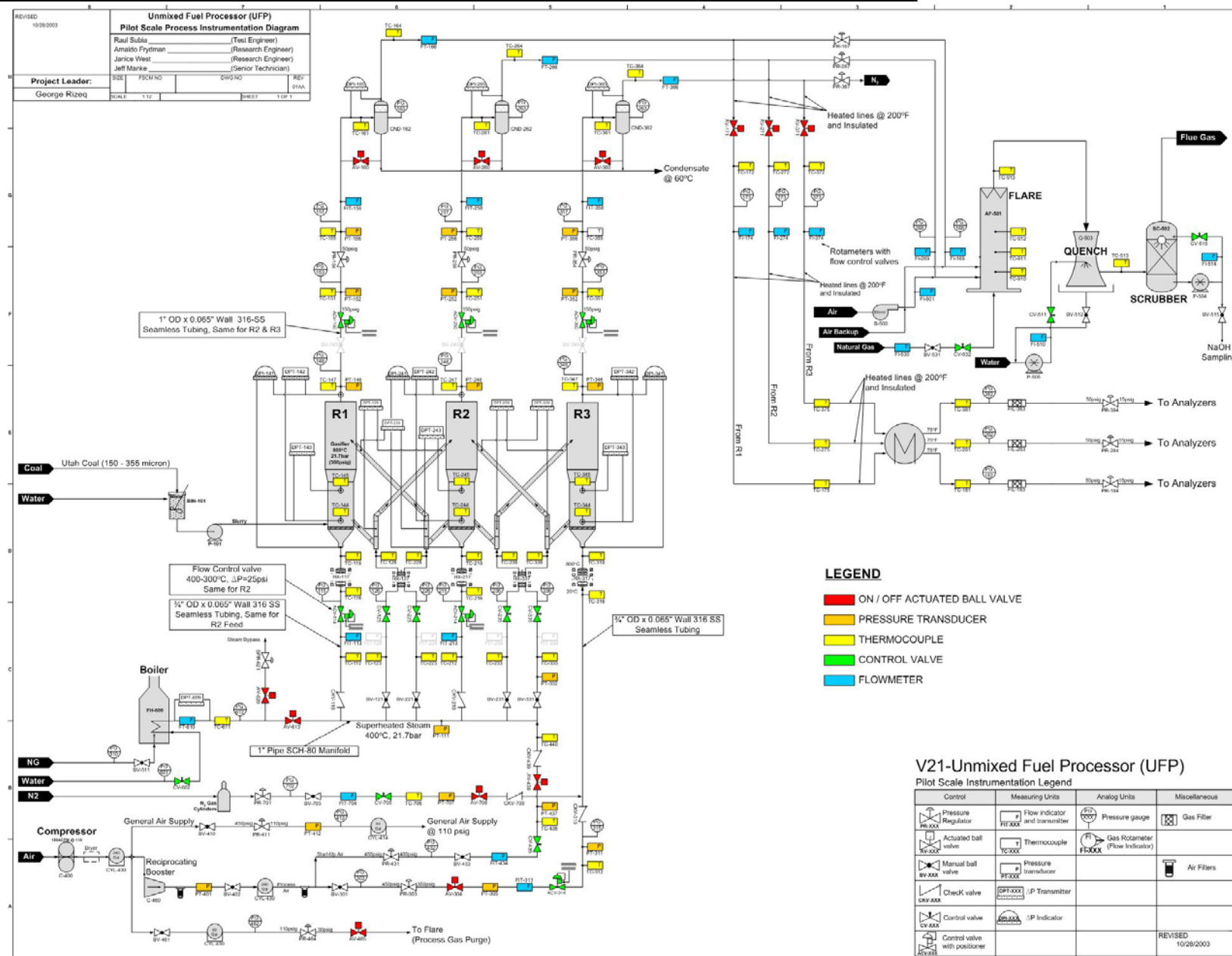


Figure 24. Process and instrumentation diagram for the pilot-scale system.

## 5.0 CONCLUSIONS

Work conducted in the third year has focused on finalizing the design of the UFP pilot plant, procuring needed equipment and instrumentation, and preparing for system assembly. Significant progress has also been made on characterizing OTM reduction behavior and coal gasification at both the lab and bench scale. In addition, process modeling efforts have provided initial pilot-scale operating conditions and integrated base cases for comparison with competing technologies such as IGCC.

The lab-scale effort in the third year has included experimental investigations into both coal gasification and oxygen transfer material (OTM) reduction behavior. Coal gasification experiments provided data on the effectiveness of the CO<sub>2</sub>-absorbing material (CAM) at removing CO<sub>2</sub> from the H<sub>2</sub>-rich product stream. Other coal gasification experiments provided insight into the impact of bed composition on UFP performance. TGA experiments were conducted to evaluate and quantify the kinetics of OTM reduction and OTM speciation as a function of temperature. This information will provide key kinetic parameters for integration in process and kinetic modeling of the system. The residence times of solids in the pilot-scale system will be set based on kinetic modeling results to ensure that sufficient time for reaction.

Bench-scale experiments conducted in the third year resulted in the development of a transfer function relating OTM reduction to GHSV and inlet concentration. This transfer function was used to identify a set of operating conditions that would provide optimized OTM reduction results. Additional testing was conducted to confirm the predicted performance at the optimized conditions, and the transfer function was updated to include all experimental results. In the expected region of operation of the pilot-scale system, the transfer function predicts reduction of up to 20% of the OTM present in the bed.

Modeling work conducted in the current reporting period has focused on development of two ASPEN process models: a model of the pilot-scale system, and a model of the full-scale UFP system integrated with a combined cycle plant. The pilot-scale UFP process model was used to assist in identifying initial pilot plant operating conditions for system shakedown. Key model input parameters include the coal feed rate, extent of coal conversion in Reactor 1, and the initial bed composition (OTM:CAM ratio). Contour plots were used to identify operating conditions for each of the three reactors that satisfy operating requirements as well as provide good performance. Key performance variables include H<sub>2</sub> purity in R1 and CO<sub>2</sub> separation in R2. The full-scale integrated UFP process model was used to estimate performance for comparison with competing technologies and to provide the inputs for preliminary economic analysis. Preliminary results obtained with the model show an efficiency improvement of 6% over IGCC. It is expected that further UFP model optimization will result in up to 10% efficiency improvement.

The pilot-scale effort has progressed beyond the design of the system and into construction and shakedown testing of individual system components. Delays in obtaining a construction and operating permit have prevented the system from being assembled as a single unit, but planning activities have continued to ensure a streamlined assembly phase. Work conducted in the third program year has involved finalizing designs, obtaining equipment, and conducting shakedown

testing of individual subsystems. In addition, care has been taken to ensure that instrumentation is in place to both allow effective control of the system as well as monitor key performance indicators.

A detailed safety analysis was conducted for the entire pilot-scale system, focusing on potential hazards and their mitigation, which have been considered in the standard and emergency operating procedures developed. The reactor designs have been reviewed, and the three reactors were manufactured and cast with two refractory layers. The systems to feed air, steam and coal were specified and manufactured. The air and coal systems have been partly assembled and tested, while the steam boiler system has been built and is being tested by the manufacturer. The solids transfer system was tested in a cold-flow model and the pilot-scale solids transfer ducts have been manufactured and cast with refractory. The emission control system, which includes an afterburner and scrubber with quench have been designed to prevent the emission of air pollutants during operation of the non-integrated system. The afterburner, quench and scrubber have been constructed and are awaiting shakedown testing. Instrumentation has been specified to meet the harsh operating conditions of the pilot plant, and is on site and awaiting assembly. The data acquisition and control system is being designed to allow safe and effective operation of the pilot plant as well as the monitoring of key variables that will be used to assess actual pilot plant performance.

Despite delays in initiating system assembly, significant progress has been made in the third program year. The pilot plant system has been designed to further establish the feasibility and performance of the UFP system. Lab and bench-scale experiments, as well as process modeling efforts have supported the pilot plant design efforts and will be used to support optimization of pilot plant operation through targeted testing of key UFP processes individually. The progress made to date has continued to establish the viability and promise of this novel technology, and planned experimental efforts aim to further establish the UFP process as a key technology that meets future power generation needs economically, efficiently and environmentally.

## 6.0 FUTURE WORK

Additional lab- and bench-scale testing will be conducted as needed to provide further insight into the rates and mechanisms of char burnout,  $CO_2$  release and OTM reduction processes. Other continuing work on UFP technology development will include the assembly and initial shakedown testing of the pilot-scale system, which will feature three fully integrated circulating, fluidized bed reactors. In addition, progress will be made on modeling tasks in support of pilot-scale system operation. Integral to all these efforts is the continuing analysis of the economics and competitiveness of the UFP technology based on experimental and theoretical findings. These tasks will aid in ensuring that the UFP system will meet the needs of the power generation industry both efficiently and economically.

### *Task 1 Lab-Scale Experiments – Fundamentals*

Task 1 activities will continue to include testing using the lab-scale high-temperature, high-pressure reactor and furnace. Kinetic tests involving coal, char, steam, air and combinations of oxygen-transfer material and  $CO_2$  absorber material will be conducted. These experimental efforts will be closely coupled with the ongoing modeling efforts to ensure that the experiments will provide information useful in model validation. Planned experimental investigations include:

- TGA experiments to evaluate the kinetics of OTM reduction in the presence of CAM, which is thought to provide a beneficial effect,
- Completion of the OTM reduction test matrix and analysis of the results to identify kinetic parameters,
- Fluidized bed experiments to quantify the residence time needed for  $CO_2$  absorption by CAM as well as the deactivation of CAM with time, and
- Fluidized bed experiments to quantify coal gasification kinetics at high pressure.

### *Task 2 Bench-Scale Facility – Design/Assembly*

This task has been completed.

### *Task 3 Bench-Scale Testing*

Future testing activities will focus on simulating pilot plant operation with regard to solids sampling and bed heat-up during startup operations as needed. These tests will provide information on the feasibility of selected solids sampling designs. Additional bench-scale tests will be conducted as needed to identify optimized operating conditions and characterize bed material performance and ash behavior. Results of these tests will be used along with lab-scale results to modify and validate kinetic and process models, as well as provide inputs for economic evaluation efforts.

### *Task 4 Engineering and Modeling Studies*

Process and kinetic models will be further developed and validated using results from testing activities. These models will also be used to provide information for pilot plant design efforts, such as setting solids recirculation rates. Ongoing economic assessments will continue to gauge the economic feasibility of the process, at different scales and considering competing technologies with additional costs associated with emerging  $CO_2$  regulations.

Future process modeling and analysis work will include the following:

- Optimization of UFP process efficiency based on the modeling and experimental results.
- Comparison of the efficiency of the IGCC and UFP technologies at various H<sub>2</sub> to electricity co-production ratios to identify the optimum operating conditions.
- Development of a robust CO<sub>2</sub> separation unit simulation using a chemical solvent
- Developing a dynamic model to analyze the start-up of the UFP technology to aid in development of an UFP technology control strategy.

#### *Task 5 Pilot Plant Design and Engineering*

This task has been completed.

#### *Task 6 Pilot Plant Assembly*

Assembly of the pilot plant has been delayed due to South Coast Air Quality Management District (AQMD) permit delays (despite early submittal of the UFP permit application). The permit to construct is expected soon, and the majority of system components are already on site and awaiting final assembly (Figure 25). A plan will be implemented for conducting shakedown testing of subsystems as they are installed, with special attention devoted to the safety and emergency shutdown systems and their integration with all equipment.

#### *Task 7 Pilot Plant Demonstration*

After the pilot plant is assembled, extensive shakedown testing will be conducted, with modifications made as needed. The operational evaluation of the UFP technology will then proceed, followed by performance testing to identify H<sub>2</sub> yields and CO<sub>2</sub> separation/release that can be achieved with thorough analysis of the experimental data.



Figure 25. Side view of pilot-scale system with three reactors, scaffolding and second-stage superheaters shown.

## 7.0 PUBLICATIONS AND PRESENTATIONS

Team members have presented the UFP concept and progress on UFP and other gasification technologies development at several conferences. These presentations and their subsequent publication in conference proceedings have generated interest in the UFP technology and helped in raising awareness of the DOE's technology development program. Educating the technical sector and industry about this emerging technology will continue to be a priority as the program progresses. The presentations are listed below.

- George Rizeq, Raul Subia, Arnaldo Frydman, Janice West, Vladimir Zamansky, and Kamalendo Das, "Unmixed Fuel Processor for Production of  $H_2$ , Power, and Sequestration-Ready  $CO_2$ ," *Twelfth International Conference on Coal Science (ICCS)*, Cairns, Queensland, Australia, November 2-6, 2003.
- George Rizeq, Arnaldo Frydman, Janice West, Raul Subia, Vladimir Zamansky, and Kamalendo Das, "Advanced Gasification-Combustion Technology for Production of Hydrogen, Power and Sequestration-Ready  $CO_2$ ", *Gasification Technologies 2003*, San Francisco, CA, October 12-15, 2003.
- George Rizeq, Raul Subia, Arnaldo Frydman, Janice West, Vladimir Zamansky, and Kamalendo Das, "Development of Unmixed Fuel Processor for Production of  $H_2$ , Electricity, and Sequestration-Ready  $CO_2$ ," *Twentieth Annual International Pittsburgh Coal Conference*, Pittsburgh, PA, September 15-19, 2003.
- George Rizeq, Raul Subia, Janice West, Arnaldo Frydman, Vladimir Zamansky, and Kamalendo Das, "Advanced Gasification-Combustion: Bench-Scale Parametric Study." *19<sup>th</sup> Annual International Pittsburgh Coal Conference*, Pittsburgh, PA, Sept 23-27, 2002.
- George Rizeq, Vladimir Zamansky, Vitali Lissianski, Loc Ho, Bruce Springsteen, Lucky Benedict, Thomas Miles, Valentino Tiangco, and Rajesh Kapoor, "Gasification-Combustion Technology for Utilization of Waste Renewable Fuels," *Bioenergy 2002: Bioenergy for the Environment*, Boise, Idaho, September 22- 26, 2002.
- Lissianski, V., Zamansky, V., and Rizeq, G. "Integration of Direct Combustion with Gasification for Reduction of  $NO_x$  Emissions," presented and published in the proceedings of the *29<sup>th</sup> Symposium (International) on Combustion*, Hokkaido University, Sapporo, Japan, July 21-26, 2002.
- George Rizeq, Janice West, Arnaldo Frydman, Raul Subia, and Vladimir Zamansky, Poster entitled: "Advanced Gasification-Combustion Technology for Utilization of Coal Energy with Zero Pollution." *29<sup>th</sup> International Symposium on Combustion*, Sapporo, Japan, July 22-26, 2002.

- George Rizeq, Janice West, Raul Subia, Arnaldo Frydman, Vladimir Zamansky, and Kamalendu Das, “Advanced-Gasification Combustion: Bench-Scale System Design and Experimental Results,” *27<sup>th</sup> International Technical Conference on Coal Utilization & Fuel Systems (Clearwater 2002)*, Clearwater, FL, March 4-7, 2002.
- R. George Rizeq, Ravi Kumar, Janice West, Vladimir Zamansky, and Kamalendu Das, “Advanced Gasification-Combustion Technology for Production of H<sub>2</sub>, Power, and Sequestration,” *18<sup>th</sup> Annual International Pittsburgh Coal Conference*, Newcastle, New South Wales, Australia, December 4-7, 2001.
- George Rizeq, Janice West, Arnaldo Frydman, Raul Subia, Ravi Kumar, Vladimir Zamansky and Kamalendu Das, “Fuel-Flexible Gasification-Combustion Technology for Production of Hydrogen and Sequestration-Ready Carbon Dioxide,” *Vision 21 Program Review Meeting*, NETL, Morgantown, WV, November 6-7, 2001.
- R. George Rizeq, Richard K. Lyon, Janice West, Vladimir M. Zamansky and Kamalendu Das, “AGC Technology for Converting Coal to Pure H<sub>2</sub> and Sequestration-Ready CO<sub>2</sub>,” *11<sup>th</sup> International Conference on Coal Science (ICCS)*, San Francisco, CA (Sept 30-Oct 5, 2001). NOTE: This conference was cancelled, but a proceedings volume was published.
- R. George Rizeq, Richard K. Lyon, Vladimir M. Zamansky, and Kamalendu Das, “Fuel-Flexible AGC Technology for Production of H<sub>2</sub>, Power, and Sequestration-Ready CO<sub>2</sub>,” *26<sup>th</sup> International Technical Conference on Coal Utilization & Fuel Systems (Clearwater Conference 2001)*, Clearwater, FL, March 5-8, 2001.

## **8.0 REFERENCES**

Tokuda, M., Yoshikoshi, H., Ohtani, M., Transactions ISII, Vol. 13, 1979, p. 357.

## **LIST OF ACRONYMS AND ABBREVIATIONS**

|          |   |
|----------|---|
| AQMD     | Air Quality Management District               |
| ASME     | American Society of Mechanical Engineers      |
| ASU      | Air Separation Unit                           |
| CAM      | CO <sub>2</sub> Absorber Material             |
| CEC      | California Energy Commission                  |
| CEMS     | Continuous Emissions Monitoring System        |
| CTQ      | Critical to Quality                           |
| DFSS     | Design for Six Sigma                          |
| GC       | Gas Chromatograph                             |
| GEGR     | General Electric Global Research              |
| GHSV     | Gas Hourly Space Velocity                     |
| HRSG     | Heat Recovery Steam Generator                 |
| IGCC     | Integrated Gasification Combined Cycle        |
| NETL     | National Energy Technology Laboratory         |
| NTI      | New Technology Introduction                   |
| OTM      | Oxygen Transfer Material                      |
| OTM-O    | Oxidized OTM                                  |
| OTM-R    | Reduced OTM                                   |
| PSA      | Pressure Swing Adsorber                       |
| P&ID     | Process and Instrumentation Diagram           |
| PID      | Proportional Integral Derivative (controller) |
| R1       | Reactor 1                                     |
| R2       | Reactor 2                                     |
| R3       | Reactor 3                                     |
| SIU-C    | Southern Illinois University – Carbondale     |
| TGA      | ThermoGravimetric Analyzer                    |
| UFP      | Unmixed Fuel Processor                        |
| U.S. DOE | United States Department of Energy            |